HHS Public Access

Author manuscript

Chem Rev. Author manuscript; available in PMC 2019 July 26.

Published in final edited form as:

Chem Rev. 2018 September 12; 118(17): 8005–8024. doi:10.1021/acs.chemrev.8b00032.

Predicting the Structures of Glycans, Glycoproteins, and Their Complexes

Robert J. Woods[*]

Complex Carbohydrate Research Center and Department of Biochemistry and Molecular Biology, University of Georgia, 315 Riverbend Road, Athens, Georgia 30602, United States

Abstract

Complex carbohydrates are ubiquitous in nature, and together with proteins and nucleic acids they comprise the building blocks of life. But unlike proteins and nucleic acids, carbohydrates form nonlinear polymers, and they are not characterized by robust secondary or tertiary structures but rather by distributions of well-defined conformational states. Their molecular flexibility means that oligosaccharides are often refractory to crystallization, and nuclear magnetic resonance (NMR) spectroscopy augmented by molecular dynamics (MD) simulation is the leading method for their characterization in solution. The biological importance of carbohydrate—protein interactions, in organismal development as well as in disease, places urgency on the creation of innovative experimental and theoretical methods that can predict the specificity of such interactions and quantify their strengths. Additionally, the emerging realization that protein glycosylation impacts protein function and immunogenicity places the ability to define the mechanisms by which glycosylation impacts these features at the forefront of carbohydrate modeling. This review will discuss the relevant theoretical approaches to studying the three-dimensional structures of this fascinating class of molecules and interactions, with reference to the relevant experimental data and techniques that are key for validation of the theoretical predictions.

Graphical Abstract

[*]**Corresponding Author** rwoods@ccrc.uga.edu.

The author declares no competing financial interest.

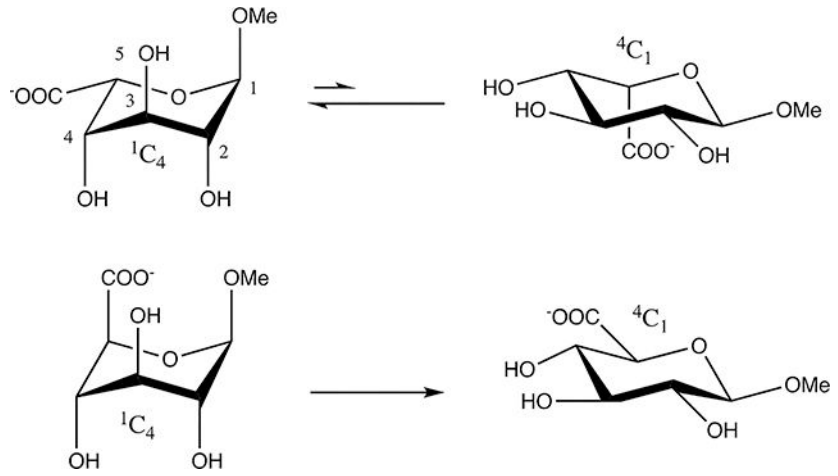

1. INTRODUCTION

Historically, the development of carbohydrate modeling methods was motivated by a desire to interpret solution data from nuclear magnetic resonance (NMR) spectroscopy in terms of three-dimensional (3D) structure.[1–5] And the approaches (protocols and force fields, for example) for modeling carbohydrates initially evolved independently from the concurrent development of biomolecular force fields for modeling proteins and nucleic acids. Carbohydrate modeling approaches such as geometry of saccharides (GESA)[6] and geometry of glycopeptides (GEGOP)[3] treated the monosaccharides as rigid, and focused on searching the conformational space defined by the glycosidic angles using Monte Carlo sampling,[5] adopting the hard-sphere exo-anomeric (HSEA) force field.[1] These early studies provided much insight into the basic properties of disaccharide linkages and were analogous in some aspects to the empirical conformational energy program for peptides (ECEPP) force field for modeling proteins, in which only the interresidue backbone angles were treated as flexible. While the protein modeling community largely adopted molecular dynamics (MD) simulations, the carbohydrate community was influenced by the HSEA/Monte Carlo strategy well into the 1990s. During the HSEA period, small-molecule modeling methods, such as the molecular mechanics (MM2/MM3) series of programs, were also adapted for use with carbohydrates.[7–12] Prior to the widespread adoption of solvated MD simulations for oligosaccharide modeling, much effort was devoted to determining the lowest potential energy (adiabatic) path for glycosidic angle rotation[13–18] or monosaccharide ring flipping,[19] in vacuo. But with the recognition of the importance of water and dynamics to oligosaccharide conformations, these methods have largely been replaced in favor of traditional biomolecular force fields.[20–24] Indeed, the development and refinement of carbohydrate force fields for AMBER,[25–29] CHARMm,[14,30–34] and GRO-MOS[20,35–39] is still ongoing, as weaknesses are discovered and corrected and limitations are removed. Advances in computer performance and software algorithms now permit conformational sampling well into the microsecond time scale, permitting convergence of MD simulations, which in turn facilitates quantitative comparisons with experimental data.[40] Such comparisons highlight the predictive strengths of current modeling methods, and identify areas that require further development.

1.1. Scope of This Review

This review will present a summary of carbohydrate 3D structure modeling. Additionally, given that the majority of mammalian proteins are modified by the covalent coupling of oligosaccharides (glycans) to their surfaces[41] and that the biological function of oligosaccharides frequently derives from their noncovalent interaction with receptor proteins, the review would be incomplete without discussing approaches to modeling glycoproteins and carbohydrate-protein complexes. Methods for computing the interaction energies of carbohydrate-protein complexes have been reviewed in detail recently[42] and will not be discussed here. A brief history of the development of carbohydrate modeling[43–45] will also be presented as some aspects bear repeating, particularly as they remain relevant to the interpretation of theoretical data and to the design and development of carbohydrate modeling methods. The review will focus on modeling methods that are extensible beyond monosaccharides to biologically relevant oligosaccharides, and will not include significant discussions of quantum mechanical approaches. Finally, emerging methods and challenges will be summarized.

2. NMR SPECTROSCOPY AND CARBOHYDRATE MODELING

As a result of the flexibility of carbohydrates, the ability to relate NMR observables to populations of oligosaccharide conformers has been at the core of their 3D characterization. In contrast, early protein modeling was largely centered on reproducing crystallographic data.[46] Initially, carbohydrate modeling consisted simply of providing plausible 3D structures for glycosidic linkages that could subsequently be combined into models of oligosaccharides.[47,48] These additive structures could then be used as models for simulations that employed NMR data as constraints.[49] However, the use of NMR data as constraints for deriving the 3D structure of a flexible molecule is problematic. Attempting to generate a 3D structure from NMR data, which arise from the contributions from more than one conformational state, will lead to a 3D structure that may be considered the average shape of the molecule. When the states are significantly different, such constrained refinements can lead to the generation of a “virtual conformation”,[50] which has long been recognized as a potential pitfall in deriving the structures of glycans from NMR data.[49,51] Consequently, it is far more appropriate to pose the question not as “What shape best agrees with the NMR data?” but instead as “What ensemble of shapes leads to the best agreement?”

From this latter perspective, the role of modeling is to generate reasonable shapes of the oligosaccharide, whose NMR properties may be computed and compared to experiment.[52,53] Scalar three-bond couplings (^3J) relate to the magnitude of the dihedral angle between the coupled spins and are often convenient to measure by NMR. Considerable effort has been dedicated to the development of ^3J-dihedral angle relationships (so-called Karplus curves)[54] that may include dependence not only on dihedral angle but also on atomic sequence and substituent patterns.[52,55–57]

2.1. Comparison to NMR Observables

One of the challenges of deriving NMR properties from gasphase energy-minimized structures is the fact that, in vacuo, the strengths of intramolecular hydrogen bonds are

overestimated, leading to inaccurate potential energy surfaces and geometries.[16,19] Nor are idealized geometries or crystallographic structures necessarily representative of solution behavior.[58,59] Explicitly solvated MD simulation has become by far the most widely used method for predicting the properties of oligosaccharides in solution. Moreover, with routinely accessible time scales entering the microsecond range, many of the earlier concerns relating to lack of conformational convergence have been removed. With advances in computer performance and in the accuracy of quantum mechanical (QM) basis sets, it is now common for Karplus relationships to be derived by fitting to QM-predicted *J*-values[60] for theoretical structures rather than by fitting to experimental data for conformationally constrained molecules. Indeed, with the ability to compute *J*-values quickly and accurately, they may be computed directly for each conformation of the carbohydrate, eliminating approximations associated with derivation of a Karplus curve.[61,62] When theoretical and experimental *J*-values are compared, it is common to compute the theoretical values for all of the structures produced from an MD simulation. This approach is particularly useful for validating the performance of a given force field or simulation protocol.[61,63] It should be noted that comparing theoretical to experimental *J*-values is not equivalent to comparing MD-generated populations to NMR-derived populations. The latter comparison may be trivial to perform from the theoretician's perspective; however, it ignores any approximations or assumptions that were applied in order to generate populations or conformations from the NMR data.[58] Given the accuracy with which *J*-values can be computed from theoretical structures, a direct comparison of these observables is likely to provide a more accurate estimate of the extent of any differences between the MD-generated structures and experimental data.[62]

2.2. Dealing with Oligosaccharide Flexibility: Scalar *J*-Couplings

For flexible oligosaccharides, achieving acceptable agreement between the theoretical conformational populations and the experimental data places extreme demands on the force field and the simulation protocol. A converged MD trajectory is not necessarily required if the purpose of the simulation is simply to identify plausible conformations that can be used to decompose the experimental data into populations. Thus, rather than attempting to achieve convergence, which is often challenging, requiring simulations that extend into the microor millisecond time scales,[61,64] a shorter simulation may identify all of the conformational states, albeit with inaccurate populations.[61,62,65] Consider the case of rotation about the C5-C6 bond in a hexopyranose.[59,62] Two homonuclear ^{3}J-values are observable, namely, between H5 and each of the prochiral H6 protons ($^{3}J_{\mathrm{H5,H6}R}$ and $^{3}J_{\mathrm{H5,H6}S}$). These *J*-values can then be decomposed into a linear combination of the population-weighted *J*-values contributed from each of the three conformations observed in the trajectory (Figure 1 and eqs 1–3).[66] Caution has to be exercised when using ^{3}J-values taken from direct measurements from spectra. When the *J*-coupling is on the same order of magnitude as the chemical shift difference between coupled spins, the splitting will not be first-order,[67] and the measured ^{3}J-value will not depend only on the torsion angles between the spins. Such a case exists for the H5—H6 coupling constants, because the chemical shift differences between H6 and H6′ are on the same order as the scalar couplings. In such cases, computer simulation of the spectrum can be performed in order to extract first-order ^{3}J-values.[68] A significant additional source of error arises in the conversion of MD-derived

torsion angles into ^3J-values. Karplus curves typically are only accurate to within about 1 Hz. For example, the ^3J-values predicted by two Karplus curves from the same MD data set differed by approximately 1 Hz.[69] A 1 Hz error in either the theoretical or experimental coupling constant can result in as much as a 30° uncertainty in the associated torsion value.

$$^3J_{\mathrm{H5-H6}R} = n_{\mathrm{gt}}{}^3J_{(\mathrm{H5-H6}R,\,\mathrm{gt})} + n_{\mathrm{tg}}{}^3J_{(\mathrm{HS-H6}R,\,\mathrm{tg})} + n_{\mathrm{gg}}{}^3J_{(\mathrm{HS-H6}R,\,\mathrm{gg})} \quad (1)$$

$$^3J_{\mathrm{H5-H6}S} = n_{\mathrm{gt}}{}^3J_{(\mathrm{HS-H6}S,\,\mathrm{gt})} + n_{\mathrm{tg}}{}^3J_{(\mathrm{H5-H6}S,\,\mathrm{tg})} + n_{\mathrm{gg}}{}^3J_{(\mathrm{HS-H6}S,\,\mathrm{gg})} \quad (2)$$

$$n_{\mathrm{gt}} + n_{\mathrm{tg}} + n_{\mathrm{gg}} = 1 \quad (3)$$

This method of decomposing ^3J-values into state populations is well established,[66] but the benefit of using MD simulation is that it eliminates one of the more contentious issues, namely, the choice (number and geometry) of the contributing states.[58] Moreover, it leverages the strengths of MD simulation (state identification), while eliminating the requirement that the populations of each state be correct. However, it requires that all of the relevant states be identified during the simulation.

2.3. Employing Additional NMR Observables: Residual Dipolar Couplings and Nuclear Overhauser Enhancements

Like scalar J-couplings, residual dipolar couplings (RDCs) provide a further NMR observable that is relatively easy to measure,[70,71] against which one can verify theoretical data or derive an experimental conformation(s).[72,73] Unlike scalar J-couplings, RDCs depend on the distance between two interacting nuclei and the angle of the bond vectors between them, relative to the external magnetic field. Due to molecular tumbling, RDCs normally average to zero; however, when the tumbling of the molecule is partially constrained, RDCs maybe observed.[74,75] RDCs provide a unique opportunity to determine the relative orientation of molecular domains, provided that there are RDCs from at least five independent bond vectors (one for each Euler angle and one for each of the principal and asymmetry order parameters).[76,77] RDC constraints are particularly useful in the determination of protein structures, where there are numerous backbone N—H bond vectors pointing at varied angles relative to each other. However, within a pyranose ring, several C—H vectors may be approximately parallel to each other, reducing the potential number of useful RDC values to characterize the shape of a monosaccharide.[78–80] In such a situation, a sparse number of RDCs may still serve a valuable role in defining the conformation(s) and dynamics of an oligosaccharide[81–84] or its orientation in a protein binding site,[79] and these may be combined with additional experimental data[72,85,86] or employed in validating the accuracy of theoretical models.[87,88] For example, in the case of heparin, an analysis of

RDCs showed, surprisingly, that despite the extreme flexibility of the iduronate ring,[89–93] interconversion between ring forms has only a modest effect on the overall shape of the molecule[82,93] (Figure 2).

Prior to the development of RDC measurement techniques, ^{3}J-values were most often augmented by nuclear Overhauser enhancements (NOEs) when determining the 3D structural properties of oligosaccharides. While ^{3}J-values and RDCs are relatively straightforward to compute accurately from 3D structures, NOEs are far more complex, because their values depend on spin relaxation, which is sensitive to both the molecular geometry (interproton distances) and the rate of internal motions as well as overall molecular tumbling.[67,94–96]

Until recently, computer speeds were not fast enough to practically compute converged values for the overall tumbling rates of oligosaccharides. Thus, for many years, the calculation of theoretical NOEs was treated qualitatively; for example, by assuming that the relative strength of the NOE between two protons was proportional only to the inverse sixth power of their internuclear separation.[97,98] A more sophisticated approach is to include spin relaxation effects arising from interactions with neighboring protons.[95,99,100] However, the results from even a full-relaxation matrix approach may fail to capture the impact of internal motion and anisotropies of molecular tumbling on the NOE. Often, converting NOEs into 3D models that include the effects of molecular motion necessitates either experimental measurement of the relevant relaxation rates, and the assumption of plausible models for analysis,[94,95,99,101,102] or their derivation by fitting to NOE intensity data.[97]

Recently, it has been shown that NOE values may be computed directly from an MD trajectory without the need to make assumptions regarding internal or global motions or molecular models,[103] provided that the tumbling of the oligosaccharide has converged. Historically, to achieve such convergence was beyond the practical limit of MD simulations on anything but the smallest systems; however, with the ability to perform long time scale MD simulations of solvated oligosaccharides, direct NOE calculations may become more viable.[103] These calculations should begin to provide insight not only into oligosaccharide structure but also on the impact of force fields, water models, and ions on molecular motions.

Finally, saturated transfer difference (STD) NMR measurements, which are based on the nuclear Overhauser effect, permit the observation of magnetization transfer from a large molecule such as a protein to the protons in a rapidly dissociating ligand, such as an oligosaccharide.[104] The STD intensities observed for the protons in the ligand are proportional to the distances between them and protons on the protein surface *when the ligand is bound to the protein.*[105] STD measurement therefore provides a particularly powerful technique for defining the orientation of an oligosaccharide in a binding site.[106,107] However, the quantitative calculation of STDs suffers from the same complexities as NOEs,[108,109] and it still remains common practice to treat STD data qualitatively.[110–114] Nevertheless, even when treated qualitatively, the ease of their measurement and the unique insight they provide into the ligand orientation in a protein complex greatly enhances their value in validating theoretical carbohydrate protein complexes. For example, STDs can aid

in discriminating between multiple theoretical poses of an oligosaccharide in a binding site generated by molecular docking (Figure 3). The simple representation of normalized experimental and theoretical NOE data, as shown in Figure 3, provides a convenient, if qualitative, assessment of the similarity of the docked and experimental pose oligosaccharide orientation relative to the protein.[111,115]

3. FIRST-PRINCIPLES PREDICTIONS OF OLIGOSACCHARIDE CONFORMATIONS

Since the introduction of modern force fields for carbohydrates, numerous analyses of data from MD simulations of oligosaccharides in solution have shown good agreement with experimental NMR data.[116] For oligosaccharides composed of monosaccharides in the six-membered pyranose ring form, there are remarkably few exceptions[117] to this capability. The current success of MD simulation of oligosaccharides reflects the evolution of force fields to the point where they now capture most of the unique properties and forces that define carbohydrate conformation. When theoretical data disagree with experiment, these important exceptions act as motivation for continued theoretical development, as well as careful reexamination of the experimental data.

Accurately predicting the 3D structure of a protein, based only on computing the interactions between amino acids (that is, from first principles), remains a largely unsolved challenge.[118] In part, this arises from the large number of potential conformations for each peptide linkage, giving rise to an exponential number of protein conformations.[119,120] In contrast, the conformational states of oligosaccharides have been well characterized (often from NMR studies or small-molecule crystallography) and appear to be guided by well-defined and predictable rules. Understanding these rules, as summarized in the essential reference *Conformations of Carbohydrates,*[121] and the underlying physics[45,122–124] has enabled accurate force fields for carbohydrate modeling to be created.[14,20,25–39] However, from a modeling perspective, the most significant property of oligosaccharides is that two-bond glycosidic linkages between pyranose rings predominantly populate only a single conformation. This can be illustrated by comparing the bond rotational energies for 2-*O*-methyltetrahydropyran (2-OMe-THP) in the equatorial (β-analogue) and axial (α) configuration (Figure 4).

In the cyclohexyl analogues, the two conformational states are determined by rotational barriers that arise principally from steric repulsions; in the THP analogues, the exoanomeric effect is present, leading to a preference only for one rotamer.[2,123,125,126] As the name implies, the exoanomeric effect has the same basis as the anomeric effect (also known as the endoanomeric effect). These effects have both been reviewed in detail[45,123,124] and are thought to originate from a favorable overlap of an oxygen lone electron pair (n_p) into the antibonding (σ^*) orbital of the adjacent C—O bond. A favorable $n_p \rightarrow \sigma^*$ interaction is dependent on the alignment (antiperiplanar) of the n_p and σ^* orbitals, which is satisfied only when the underlying atomic geometry is in a particular conformation. In pyranoses, in the $^4C_1$ ring form, the optimal anomeric effect [between the lone pair of the ring oxygen (O5) and the C1-O1 bond] occurs when the C1-O1 bond is in the axial configuration; this

preference is in contrast to expectations based solely on steric arguments. Within the O5—C1—O1 atomic linkage, the lone-pair electrons of the exocyclic O1 atom also have the ability to overlap with the σ^* orbital of the endocyclic C1—O5 bond, provided the orientation is favorable. This property gives rise to the exoanomeric effect, which is the preference of the ϕ glycosidic angle (O5—C1—O1—C) to adopt a ±gauche orientation with respect to the ring oxygen (Figure 5). As the anomeric effect depends on the configuration at C1 (the anomeric carbon atom), which is generally unchanging in a monosaccharide, it is arguably the exoanomeric effect that has the more profound impact on the 3D structure and dynamics of oligosaccharides.

If the dominance of the exoanomeric effect in defining the conformation of the ϕ glycosidic angle is assumed, and also that the Ψ angle [C1—O1—Cx—C(x − 1)] will be determined by steric effects,[127] it is possible to predict the conformation of most two-bond glycosidic linkages.[17,18,47,48,128–131] A simple rule for remembering the conformational preferences of the ϕ and Ψ angles between pyranose rings is that the C2—C1—O1—Cx ϕ angle will be approximately 180° and the C1—O1—Cx—Hx Ψ angle will be approximately 0°. All current carbohydrate-specific force fields typically use a combination of steric, electrostatic, and torsional energy terms to capture the underlying physics of these interactions. This raises a question: “If glycosidic linkages generally[48] (but not always)[132] adopt only one conformation, why are oligosaccharides frequently said to be highly flexible?”

3.1. Origin of Oligosaccharide Flexibility

In part, the flexibility of oligosaccharides arises from the fact that, unlike globular proteins, they rarely exhibit secondary structural elements that are stabilized by strong interresidue hydrogen bonds, nor do they fold into stable tertiary structures. While internal hydrogen bonds between hydroxyl groups may play a role in stabilizing a conformational state, they are not thought to be responsible for driving changes in glycosidic torsional states.[133] The ability of water to disrupt internal hydrogen bonds results in glycosidic linkages exhibiting significant motions (often ±~15°) around a single state.[97] These librations may, however, be considerably dampened in regular polysaccharides, such as cellulose, that form strong interchain interactions.[134–136]

Additionally, not all glycosidic linkages involve only two bonds: some contain three, or even more. A notable example of a three-bond sequence is the 1—6 linkages found in the highmannose type of mammalian glycans (Figure 6).

The additional rotatable bond in a 1—6 linkage (characterized by the ω angle O6—C6—C5—O5) naturally increases the flexibility of the linkage, although again, fortuitously for modeling, not by as much as might be expected. Surprisingly, whenever the C6 atom is part of a manno- or glucopyranosyl residue, the ω angle populates only the two gauche rotamers of the three plausible staggered orientations.[58,59,62,137–139] This observation has been attributed to the presence of a “gauche effect” between the vicinal O6 and O5 oxygen atoms.[59,62,122] However, the origin of the gauche preference in carbohydrates appears to be more complex than the simple stereoelectronic orbital overlaps that define a canonical gauche effect.[140–142] When the C6 atom is part of a galactopyranose residue, the ω angle may populate all three staggered rotamers.[62,137,138] The structural difference between manno/

glucopyranose and galactopyranose is the configuration of the hydroxyl group (O4) at C4; it is equatorial in the first pair of monosaccharides and axial in the latter. Thus, the gauche effect depends not only on the relationship between the vicinal O6 and O5 but also on the configuration of O4. The physics behind this effect has been shown to depend on 1,3-diaxial repulsions between the oxygen atoms, which are enhanced when water disrupts the otherwise stabilizing internal hydrogen bonds.[62,122] Additionally, the more chaotropic the solvent, the less the gauche effect is manifest.[62,143]

Unlike most two-bond glycosidic linkages, which liberate around a single average value, the ω angles may interconvert between the + and − gauche states. Thus, despite the fact that a high-mannose glycan contains 10 glycosidic linkages, including two 1–6 linkages, to a first approximation there are only four stable conformations, each populated to differing extents.[9,144] It is for these reasons that representative models of oligosaccharide conformations can be readily generated. The initial models generated from the rules of carbohydrate linkage preferences are primarily useful for qualitative or visual assessment of the oligosaccharides (Figure 7). To obtain more quantitative insight, such as an estimation of the population of each rotamer, or of their NMR properties, requires subjecting them to a more sophisticated analysis, such as MD simulation.

3.2. Role of Ring Flexion in Oligosaccharide Dynamics

On the basis of NMR and crystallographic data, the great majority of pyranose monosaccharides, particularly when present in oligomers, adopt a single ring conformation (pucker) in solution and in the solid state. This has aided carbohydrate modeling immensely, as it means multiple ring shapes need not generally be considered. Moreover, until recently, the microsecond time scales[148] required to observe ring flipping were generally inaccessible. This is no longer the case. It is now feasible to perform MD simulations for sufficient time to observe ring flipping; however, determining accurate populations of the ring forms may still require extremely long simulation times to converge.[64] Among pyranoses, the poster child for ring flipping is α-L-iduronic acid (IdoA), a very well-studied component of heparin and heparan sulfates (Figure 8). The α-form (axial at C1) has a strong anomeric effect and can apparently tolerate three axial hydroxyl groups (Figure 8). The equilibrium between the $^1C_4$ and $^4C_1$ ring forms of IdoA has been studied for many years;[117,149] it is complex to quantify, but the $^1C_4$ form appears to be favored.[117,149] In comparison, the closely related C-5 epimer glucuronic acid (GlcA) exclusively prefers the $^4C_1$ ring form. The preference in IdoA for the $^1C_4$ form is unlikely to arise solely from the anomeric effect. Clearly the presence of the equatorial carboxylate has a strongly stabilizing influence (or in the axial configuration is strongly destabilizing).

Although the ring conformations of pyranoses are often thought to populate only one state, caution should be exercised with that assumption. Such conclusions are often based on the interpretation of NMR scalar ^3J-couplings, and as with any experimental method, there are limits to the sensitivity of the detection method. A low population of another conformational state may well remain undetected, given the additional complexities and approximations associated with converting NMR data to conformer populations. A possible example of such a situation may be seen in the case of *N*-acetylglucosamine (GlcNAc), which is generally

accepted[150] to exist exclusively in the $^4C_1$ conformation in solution. However, MD[132,150] and crystallography[132] suggest that it may undergo significant but rare ring flips that may facilitate specific biological recognition processes.

Unlike pyranoses, when a sugar exists in a five-membered form (furanose), the ring is notoriously flexible. Well known furanoses include the fructose ring in sucrose and the ribose and deoxyribose rings in RNA and DNA. Furanose rings are not found in mammalian glycans, but they are widespread in bacteria, fungi, and plants. Long MD simulations have been used to characterize ring flipping in furanoses[29,151] to probe their physical origin,[29] and to evaluate force field performance.[29,151] Access to the microsecond time scale is essential for achieving convergence in many MD properties of relevance to oligosaccharides and will no doubt lead to discovery of the limits of force fields developed prior to this advantage.

3.3. Impact of Charged Moieties

Many oligosaccharides are modified by charged moieties, such as the sulfated oligosaccharide heparin, discussed earlier. Electrostatic repulsion between sulfate groups has been proposed to be responsible for ring conformational changes[90] and the formation of favorable hydrogen bonds between hydroxyl groups and sulfate moieties (Figure 9).[152,153] Somewhat in contrast, a theoretical charge mutation study, in which the partial charges on sulfate moieties were set to zero, indicated that steric repulsions between sulfate groups were as important as unfavorable electrostatic forces, at least in one example.[152]

The simplistic view that carbohydrates that contain carboxylate, phosphate, or sulfate groups are anionic ignores the fact that in most environments such molecules should be thought of as salts, by virtue of the fact that their net charge is neutralized by the presence of counterions, most typically sodium. And indeed, simulations of heparin disaccharides performed with and without neutralization by sodium ions show modest but significant differences in the conformations of the glycosidic linkage.

Other than heparin/heparan sulfate and related glycosaminoglycans, common monosaccharides that contain negatively charged groups include the sialic acids, which can also polymerize. Poly-2–8-sialic acid (PSA, Figure 10) is a component of neural cell adhesion molecules (NCAM glycoproteins), and its conformation has been the subject of several studies.[154–157] This molecule contains four rotatable bonds in the glycosidic linkage (ϕ, Ψ, and two ω angles), and NMR/MD studies of its trisaccharide constituents show that the internal ω angles are relatively stable, resulting in a well-defined structure (Table 1).[65] It has also been recently shown by NMR and MD simulations that the configuration of the free reducing terminus can impact the rotamer populations of the immediately preceding glycosidic linkage.[158]

However, full-length PSA is far more elongated than the well-characterized trisaccharide,[65] and some dispute exists as to whether the larger oligosaccharides populate multiple conformational states[65,159] or adopt a regular helical structure.[156,157,160] On the basis of the enhancing effect of cation concentration on PSA-antibody binding, it was concluded that divalent cations and polyamines may play significant roles in regulation of the PSA epitope

presentation in vivo.[161] Thus, the range of results and opinions regarding the shape of PSA may well stem from an incomplete understanding of the role of counterions. This suggests an important opportunity for long-scale MD simulations. However, determining the parameters for divalent cations remains an area of active development,[162,163] and this raises an important but often overlooked issue. A biomolecular force field not only must be internally consistent but also must be balanced with regard to the strengths of the interactions between biomolecules, solvent (water), and ions.

4. ROLE OF COUNTERIONS AND WATER MODELS

4.1. Charge Neutralization

When simulating charged systems, it is typical to neutralize the solute by the addition of counterions, prior to solvating with water molecules. In the case of proteins that are only marginally stable, it has been shown that omission of charge neutralization leads to denaturation during MD simulation.[164] Given the high flexibility of oligosaccharides, a simulation of a polyionic oligosaccharide performed in the absence of counterions would also be expected to result in irrelevant conformations and populations. It is thus important to model, and practically consider, polyionic oligosaccharides as neutral salts. This conclusion has subtle implications for the interpretation of 3D structures and intermolecular interactions of molecules, such as glycosaminoglycans and PSA, which are still commonly referred to as polyanionic species.

4.2. Ion Coordination

As seen in the case of PSA,[165] the presence or absence of calcium ions can impact the 3D structure of an oligosaccharide, and it is well-known that the interaction of other anionic polysaccharides (such as alginate) with divalent metals can lead to gel formation.[166] This is not surprising, given the ability of Ca^{2+} to coordinate with multiple hydroxyl groups in a carbohydrate,[167,168] although the specific structure of the coordination complexes may vary depending on the ion.[168] Many proteins, such as C-type lectins, exploit the affinity of carbohydrates for calcium by evolving a calcium-binding domain in the protein that serves to anchor the carbohydrate in the binding site.[169–177] Calcium ions have also been proposed as a weak glue that enhances the interactions between two oligosaccharides, as in the case of the calcium-mediated binding between two Lewis X antigens.[178] Interestingly, PSA forms a 1:1 complex (Neu5Ac/Ca^{2+}) in which the calcium ion coordinates to both the carboxylate and the glyceryl side chain within a single Neu5Ac residue.[167,179]

While the MD simulation of an isolated oligosaccharide is now straightforward, the study of calcium-dependent interactions or aggregation is far more complex. At present, it is unclear whether a long simulation with arbitrarily placed divalent ions will converge, and if so, would converge to the same ensemble of structures if the MD is repeated. There is also a paucity of experimental structural data against which to validate the theoretical models.[178] Thus, despite the biological importance of calcium—carbohydrate interactions, additional experimental and theoretical studies will be required to establish the accuracy of MD simulations of these systems. Although significant for many diseases, from cystic fibrosis[180,181] to endocarditis,[182] the complex calcium-mediated aggregation of

polysaccharide biofilms represents a particularly challenging class of structure to model.[183,184]

4.3. Water—Water versus Water—Carbohydrate Interactions

Carbohydrate—carbohydrate interactions have been postulated to exist and have been probed experimentally.[185–193] For example, atomic force microscopy revealed equally strong adhesion forces between glycan molecules (190—310 pN) as between proteins in antibody—antigen interactions (244 pN).[194] But to date these systems have received little computational attention.[189] While spontaneous carbohydrate aggregation naturally occurs when carbohydrates crystallize at high concentrations, in MD simulations at lower concentrations unexpected aggregation has also been reported to occur, depending on the water model employed in the simulation.[195] Water models are generally developed to reproduce the properties of water and are not necessarily optimized for interactions with solutes. Rather, it is the force field of the solute that is usually "tweaked" to perform optimally with a given water model.[196] The transferable intermolecular potential three-point (TIP3P)[197] water model is one of the simplest descriptions (rigid bonds and angle, fixed partial charges, van der Waals only on the oxygen atom). Innumerable successful simulations of proteins, nucleic acids, and carbohydrates have been performed in TIP3P water. However, it is not a perfect water model.[198] Other models, including TIP5P, which is still rigid but includes lone-pair electrons, better estimate the viscosity of water[199,200] and reproduce the temperature of maximum density of water.[198,201] To the extent that the water model serves principally to provide a damping force on electrostatic interactions or a compressive force on the solute,[135] the fact that it is not an optimum model for all properties of water may not harm the simulation. However, in some cases, the water model can impact the outcome of the simulation. Both the CHARMM36 and GLYCAM06 force fields have been reported to display excessively strong amino acid-sugar interactions.[202,203] Additionally, with GLYCAM06, it is possible to detect aggregation of oligosaccharides in TIP3P water at oligosaccharide concentrations that are lower than the point at which aggregation should occur.[196,204] This artifact disappears when the simulations are performed in the TIP5P water model.[204] When applied to deriving an electrostatic model for water, the approach used for deriving partial atomic charges in GLYCAM06 led to a water model that was similar to TIP5P,[205] suggesting the origin of the better performance of GLYCAM06 in TIP5P stems from balanced electrostatic interactions. Furthermore, when three water models (TIP3P, −4P, and −5P) were examined, only TIP5P reproduced the known preference of a key water molecule[169] to occupy a conserved water-binding site in the complex of the lectin concanavalin A and a trisaccharide.[170]

5. MODELING GLYCOPROTEINS

In vivo, oligosaccharides are most often physically attached to either a protein (glycoprotein, gp) or a lipid (glycolipid), and these are generally embedded in a cell membrane.[206] The immobilization of the glycan may restrict the number of conformational states that it can adopt, and it certainly alters the manner in which the glycan can interact with other receptors.[207–210] It is essential to understand the impact of glycan presentation on recognition,[210–213] whether relative to a biological surface or to a man-made surface, such

as a glycan array, in order to advance from studies of small oligosaccharides in vitro (or in silico) to biologically relevant interactions.[96,214,215] While glycosylation may not alter the overall fold of the protein,[97] the covalent attachment of glycans to a protein has been shown to dampen the protein backbone dynamics,[216–218] with potential consequences for protein stability[219] and enzyme activity.[220] Additionally, there are important examples in which glycosylation alters the conformational distributions of protein loops, including the case of the V3 loop in gp120[221–223] and the Fc domain in immunoglobulin G antibodies.[224–226] Fortunately, the most serious hurdle (computational demand) to simulations of glycoproteins is becoming less and less of a limitation. There is no intrinsic problem in generating a model of a glycoprotein (based on an experimental or theoretical structure of the protein and a structure, derived a priori, for the glycan), and subjecting it to MD refinement. There are, however, several practical issues that must be addressed. Glycans are often deliberately removed from proteins to aid in protein crystallization; when they are present, because of the flexibility of the glycans, typically only the two or three monosaccharides closest to the protein surface are resolved. A potential mistake made by nonexperts is to assume that the monosaccharide residues present in the crystal structure represent the biologically relevant glycan. This may not be the case, as often the outer branches on the glycan are not resolved in the diffraction data. The first step in modeling glycoproteins is to identify the sites that should be glycosylated; the second is to choose the glycan to model at that site.

5.1. Dealing with Glycan Heterogeneity and Partial Occupancy

One of the most challenging aspects of glycoprotein modeling arises from the fact that naturally occurring glycoproteins exist as an ensemble of glycosylated variants (glycoforms) that differ not in the protein sequence but in the composition of the glycans that are present at each glycosylation site.[227] Enzymatic processing of the glycans in the Golgi and endoplasmic reticulum, and even by exogenous glycosidases, leads to microheterogeneity in the composition of the glycans at each site.[228,229] This information is generally not included in the crystallographic structure file, and thus the modeler must decide which glycans to add to each site. Moreover, the site occupancy (macroheterogeneity) may vary, depending on the cell type and glycoprotein production conditions.[228,229] Although it is possible to generate models by selecting the glycans from glycomic data,[230] modeling glycoproteins requires assumptions or hypotheses to be made regarding the key glycoforms.[213]

The importance of glycoprotein micro- and macroheterogeneity cannot be overstated, given that the motivations for modeling glycoproteins include understanding the effects of glycosylation on protein function,[231] defining the ability of the glycan to shield a pathogenic protein from immune recognition,[232–239] and rationalizing the recognition of clusters of glycans on the glycoprotein surface.[230,240,241] As an example, the glycans on the surface antigen glycoproteins of the human immunodeficiency virus (HIV) shield it from human immune detection (moderating its immunogenicity). Shown in Figure 11 is the glycan shield present on the trimeric glycoprotein complex of gp120 and gp41;[232,242] understanding the relationship between surface glycosylation and biological function, and vaccine design, has provided important motivation for glycoprotein modeling.[221,232,243,244]

6. MODELING CARBOHYDRATE-PROTEIN COMPLEXES

Much has been learned regarding the relationships between linkage positions and hydroxyl-group configurations and oligosaccharide 3D structure, to the extent that accurate prediction of the conformation of oligosaccharides is now routine. Nevertheless, the biological function of most glycans involves, at one stage or another, their interaction with a receptor, typically a protein.[206,245] The ability to characterize carbohydrate-protein complexes is therefore at the forefront of understanding the function of glycans in biology. This arena has long been dominated by protein crystallography, and to a lesser extent by NMR methods.[246] Neither of these methods is high-throughput, presenting an important opportunity for theoretical modeling.[247] Fortunately, from a modeling point of view, in the majority of examples, receptor proteins, at least those that are not enzymes, appear to have evolved to bind to the most populated solution conformation of the oligosaccharide (Figure 12).[248,249] Given a structure for a receptor protein cocomplexed with an oligosaccharide, there are no particular challenges associated with its simulation, although there are some important details to consider.

6.1. Hydrogen Bonds

Hydrogen bonds are a hallmark of all protein—carbohydrate complexes; however, these are not observed explicitly in crystal structures (the hydrogen atoms are rarely resolved) but are only inferred from the distances between electronegative atoms. Adding the missing hydrogen atoms is often straightforward and based on analytical placement, with some important exceptions. Additionally, at physiological pH, the ionizable side chains of proteins and oligosaccharides are assumed by default to be charged. However, with carbohydrate ligands, the hydrogen bonds inevitably involve hydroxyl groups, which may be either donors or acceptors, and so the location of hydroxyl hydrogen atoms can be ambiguous in a complex. The same issue arises with waters of crystallization. Nor is the protonation state of a histidine residue necessarily known or uniquely inferable in the complex. One simple remedy is to restrain only the non-hydrogen atoms in the carbohydrate, protein, and waters of crystallization during an initial MD simulation phase, allowing the hydrogen atoms to reorient to their preferred locations, prior to releasing the constraints.

6.2. pH Effects

But what if the structure of the complex was not determined at physiological pH, or what if the biological activity occurs at lower or higher pH? A recent analysis of the binding of heparin fragments to the heparin receptor protein (CCL5) serves to illustrate the importance of pH effects in MD simulations of carbohydrate—protein complexes.[250] To avoid stochastic aggregation, it is common practice to study protein—glycosaminoglycan complexes at low pH (pH = 3—4). Initial simulations of the heparin—CCL5 complex that assumed a neutral pH failed to reproduce the cocrystal structure; the ligand was unstable and relocated from a presumed binding groove to a nearby loop where the sulfate moieties interacted with basic amino acids [arginine (R) and lysine (K)]. Only when the protein aspartate, glutamate, and histidine residues and the carbohydrate uronic acids were treated as protonated was the MD of the complex stable in the crystallographic pose.[250] The take-home message here is that, the ionization states of the protein residues can significantly alter the preferred

oligosaccharide binding site. But even more importantly, the artificially low pH employed during cocrystallization,[251,252] appears to have biased the structure of the cocomplex. Further simulations under physiological conditions and experimental point mutagenesis confirmed that the biologically relevant binding mode indeed involved the basic amino acids in the loop domain.[250]

6.3. Errors in Protein Data Bank Data

Although several programs exist to check the accuracy of protein structures before and after deposition into the Protein Data Bank (PDB), remarkably little curation is performed on the carbohydrates in these structures. This has led to a very high level of errors, either in the coordinates or in other aspects.[248,253,254] Just as it is well-known that the orientation of the terminal amides of glutamine and asparagine may be ambiguous in protein structures, it is worth noting some of the issues that abound in the carbohydrate ligands. These include flipped amides (most notably in sialic acid residues) and severely distorted ring shapes. These problems may resolve themselves during an MD simulation, but then the modeler is left with the task of justifying why the model disagrees with the crystal structure. The old adage—that everyone trusts an experimental result except the person who performed the experiment, while no one trusts a theoretical result except the person who performed the calculation—would perhaps be less onerous on the theoretician if the experimental data were better curated! But what to do if a crystallographic cocomplex is not available at all?

7. DOCKING OLIGOSACCHARIDES TO PROTEINS

Perhaps the most challenging task in carbohydrate modeling is generating plausible structures for carbohydrate—protein complexes in the absence of crystallographic data.[247,255,256] Yet the ability to do this accurately is arguably what would most rapidly advance the development of carbohydrate-mediated disease interventions. Whereas accurate prediction of the conformational properties of oligosaccharides is now relatively straightforward' the same cannot be said for prediction of their complexes with proteins. Although much progress has been made' the community of carbohydrate modelers and structural biologists might benefit significantly from increased participation in the Critical Assessment of PRediction of Interactions (CAPRI) competition. CAPRI is aimed at evaluating the ability of docking protocols to correctly predict the 3D structures of cocomplexes.[257] The experimental coordinates of the ligand are kept secret until after the double-blind competition' thus offering an objective opportunity for the assessment of docking protocols.

7.1. Preparing the Receptor and Validating the Model

Just as it is important to prepare a protein for MD simulation by adjusting hydrogen positions and checking for flipped amino acid side chains (glutamine, asparagine).[258] the outcome of docking will also benefit from careful preparation ofthe protein. Until recently,[256] no docking protocols included the conformational preferences of carbohydrate ligands, and it remains good practice to test the applicability of any chosen method prior to beginning a project. A common validation test or positive control is to ensure that the docking algorithm can correctly predict the pose of a carbohydrate ligand relative to a

known cocomplex. If the intent is to treat some part of the ligand as flexible (the glycosidic linkages, perhaps, or the hydroxyl groups), the impact of this on the positive control should also be evaluated. Regardless of the successful reproduction of the positive control, it would be naïve to assume that it will also succeed on a different protein and or with a different ligand. Fortunately, there are a number of additional steps that can be taken to help increase the likelihood that the docked complex is accurate, including indirect experimental validation.

7.2. Flexible or Rigid Receptor Docking

Docking produces two results: one is a list of ligand poses that are theoretically optimally aligned to the protein surface, and the other is an estimate of the interaction energy for each pose. It is common practice to treat the protein as rigid and consider flexibility only within the ligand.[259,260] This can be a severe approximation, as it eliminates the possibility of treating induced fit in the protein. However, unless the docking protocol explicitly treats the conformational preferences of the glycosidic linkages,[256,261] introducing protein flexibility is likely only to provide additional opportunities for generating poses with incorrect conformations of the oligosaccharide. This likelihood is enhanced by the fact that CH—π interactions, which are commonly seen between monosaccharides and aromatic amino acid side chains,[262,263] are not explicitly treated in current biomolecular or docking force fields.[264] If the protein side chains are to be treated as flexible, it may be preferable to keep the carbohydrate rigid to reduce the number of degrees of freedom and thus enhance the sampling of nearly correct poses. Fortunately, it has been shown that in the majority of carbohydrate-containing crystal structures, with the potential exception of enzymes, the oligosaccharide adopts low-energy solution-like conformations (Figure 12).[248,249]

In the case of glycans, the obvious coordinate to permit to be flexible would be the glycosidic torsion angles, as these directly impact the 3D shape of the ligand. As illustrated in Figure 4, glycosidic linkages have well-defined conformational preferences that limit the potential number of conformational states. As most docking programs are unaware of the conformational preferences of ligands, carbohydrate docking can lead to unreasonable distortions of the ligand shape.[256] While the correct pose may be present among the docking output, it is far from certain to be the top-ranked pose.[256,265–268] Thus, it is good practice to objectively detect and remove unlikely conformations generated by docking prior to proceeding with further analysis.[249] Other advances have focused productively on exploiting the observation that the hydroxyl groups in monosaccharides often displace bound waters in the protein binding site.[171,269,270] Thus, an awareness of the preferred water sites can be employed to guide carbohydrate docking.[271] Docking may be performed with a limited number of the protein positions permitted to be flexible, but at present it cannot generally treat monosaccharide rings flexibly. For the majority of oligosaccharides this is not a significant limitation; however, when docking oligosaccharides that contain flexible rings, such as furanoses, or certain pyranoses (IdoA), the lack of ring flexibility may be an important limitation. At present the options are (i) to generate and dock multiple shapes of an oligosaccharide as a function of ring shape, a process that is automated in the RosettaCarbohydrate package,[261] or (ii) to perform an MD simulation of the docked

complex. This latter approach is frequently seen in docking studies, as it also permits the protein to move and reintroduces water molecules.[110,111,255,272]

7.3. Noncrystallographic Approaches to Validation

Regarding experimental validation, in the absence of a crystal structure, STD NMR data (already discussed) can provide important corroboration.[109–111,273] Additional experimental data that may be useful for validation of the docked pose include an analysis of the impact of point mutagenesis or alanine scanning on glycan recognition.[110,297] If mutating a residue to alanine impacts ligand binding, then the assumption is that the residue is likely to be proximal to the ligand. The docked model should be consistent with the effects of such mutations. Prior to the widespread availability of protein crystallography, chemical modifications to the ligand, such as O-methylation or deoxygenation, were employed to identify those hydroxyl groups involved in hydrogen bonds with the protein.[274] When available, such data can also be used to validate proposed cocomplexes. More recently, glycan array screening (GAS)[275–279] has become widely used to identify binding partners for a given protein, from an array of on the order of 500 glycans. However, the specificities observed (oligosaccharides that bind and those that do not) can also serve to identify the acceptable poses from docking.[111] All binding ligands in the glycan array that share the same motif as that docked to the protein (the minimal binding determinant) should align similarly in the protein binding site,[275] whereas nonbinders that share the same motif might be expected to lead to clashes with the protein surface.[111,275] The optimal pose from docking should enable a rationalization of both the binding and nonbinding ligands from GAS. At least one online tool (Gly-Spec, www.glycam.org/gr) has been developed to facilitate such comparisons.[280]

8. ISSUES AND PROSPECTS

In this final section, we will summarize those areas of carbohydrate modeling that remain or have emerged as challenges and provide some general guidelines. Conformational sampling in MD simulations has historically been insufficient to claim convergence, but with routine access to microsecond time scales, sufficient sampling can now often be achieved. Certain systems, such as those displaying large domain motions,[96,224] will still require longer times or alternative approaches in order to converge, and the extent of convergence should always be examined. That said, a converged value represents the limit of the performance of a given force field and water model, and the model should not be mistaken for reality. More complex issues include optimal parameters for the modeling of ions, with one interesting recent proposal being to model Ca^{2+} as an ion with bound water molecules.[163] Other remaining issues include the potential need to include CH-π interactions explicitly, as well as charge polarization. This latter aspect has received considerable attention,[281–287] but broad adoption within the biomolecular modeling community has been slow.

The GLYCAM force field was introduced in 1995,[288] followed by the report of a 1 ns solvated MD simulation of a high-mannose oligosaccharide (Man-9),[97] which took approximately 1 month of real time to obtain on a supercomputer. At the time, this represented the state of the art, and to play on the words of Neil Armstrong, it could be

described as being one small step for Man, one giant leap for Man-9. A comparable data set could now be obtained in hours running on a personal computer. However, to achieve converged sampling of rotational transitions for some glycosidic linkages, especially those with three or more bonds, requires time scales well into the microsecond regime.[289] With optimized hardware and MD code, it is even possible to extend into the millisecond time scale,[290] although this is far from routine. MD over shorter time scales may nevertheless be employed to objectively identify relevant conformational states,[61,62,65] which can be used in the interpretation of NMR data, but the essential question remains: “How long is long enough for an MD simulation?”

The answer to this question depends on the lifetimes, or transition frequencies, of the motional properties that are under consideration. With the ability to achieve convergence of many structural properties by MD, simulations have moved from being largely retrospective to predictive.[40,289] As well as facilitating the prediction of conformational populations,[29,65] the ability to achieve convergence greatly enhances the power of MD simulations as a tool for force field validation.[28,33,40,73,291]

Most current biomolecular force fields have similar fundamental formulations and may be said to have reached (or nearly so) a first-order approximation for modeling molecular structures. More complicated force fields drastically increase the real time required for an MD simulation to achieve convergence. Quantifying the improvements offered by such second-order evolutions of a force field are difficult to assess until convergence can be obtained. Viewed in hindsight, theoretical improvements in carbohydrate modeling have led to a much greater depth of understanding of the properties of these complex molecules and to the ability to quantify many key features, but they have not profoundly altered many of the conclusions derived from extremely approximate early models, at least regarding their conformational preferences. Fortunately, the ever-increasing capability of computers and software enables the performance of increasingly complex force fields to be evaluated.

A unique challenge in modeling highly glycosylated glycoproteins is the generation of an initial model that does not contain glycan-glycan or glycan-protein collisions. The glycans are frequently added to the protein with no prior knowledge of their orientation relative to the surface; for multiple glycans in close proximity, severe overlaps can be generated that may not be resolved by simple energy minimization. Thus, at present, some element of manual adjustment of glycan orientation may be required prior to initiating simulations. To remove any resulting artifacts and obtain viable conformational distributions for the glycans, one approach is to subject the glycoprotein to long MD simulations.[213] Improvements in glycan placement algorithms[292] are going to become increasingly important, as more glycoproteins become the object of structural analysis.

Noncrystallographic methods applicable to validating carbohydrate modeling include fast photochemical oxidation of proteins (FPOP), which offers the potential to provide relatively high-throughput detection of protein residues that are shielded from solvent.[293] As the technique matures, FPOP data offer the possibility of generating data for the protein that are complementary to ligand STD NMR data, in the sense that the FPOP data can be related to the surface residues shielded in a complex.[208,294] Additionally, the rapidly advancing

resolution capabilities of cryo-electron microscopy offer an exciting additional source of experimental data to validate and develop theoretical models of glycoproteins.[295,296]

ACKNOWLEDGMENTS

The author gratefully acknowledges the contributions from colleagues and group members, past and present, without whose efforts this review would not be possible.

Biography

Robert Woods received his undergraduate training at Queen's University, Canada, in engineering chemistry, followed by a Ph.D. in synthetic and theoretical carbohydrate chemistry at the same institution. His postdoctoral training included a period of three years in the Glycobiology Institute at the University of Oxford, followed by a year at the National Research Council in Canada. In 1995 Professor Woods took a position as assistant professor at the Complex Carbohydrate Research Center in the Department of Biochemistry at the University of Georgia, where he is currently a full professor and Director of the Computational Glycobiology Laboratory. From 2008 to 2014 he was jointly affiliated as a full professor at the School of Chemistry at the National University of Ireland, Galway. He is also the President of Lectenz Bio, LLC, a biotech company located in Athens, GA. Professor Woods serves on the editorial boards of the journals *Glycobiology* and *Journal of Biological Chemistry*. His research interest is in the general area of molecular recognition, with a focus on carbohydrate-protein interactions related to human diseases. His group uses a range of approaches, from computational chemistry and chemical synthesis to molecular biology and biophysics. The Woods group maintains an extensive set of carbohydrate-modeling tools on the GLYCAM Web site (www.glycam.org).

REFERENCES

(1). Lemieux RU; Koto S The Conformational Properties of Glycosidic Linkages. Tetrahedron 1974, 30, 1933–1944.

(2). Thogersen H; Lemieux RU; Bock K; Meyer B Further Justification for the *Exo*-Anomeric Effect. Conformational Analysis Based on Nuclear Magnetic Resonance Spectroscopy of Oligosaccharides. Can. J. Chem 1982, 60, 44–57.

(3). Stuike-Prill R; Meyer B A New Force-Field Program for the Calculation of Glycopeptides and Its Application to a Heptacosapeptide-Decasaccharide ofImmunoglobulin G_1. Eur.J. Biochem 1990, 194, 903–919. [PubMed: 2269309]

(4). Poppe L; Stuike-Prill R; Meyer B; van Halbeek H The Solution Conformation of Sialyl-Et(2 6)-Lactose Studied by Modern NMR Techniques and Monte Carlo Simulations. J. Biomol. NMR 1992, 2, 109–136. [PubMed: 1422148]

(5). Peters T; Meyer B; Stuike-Prill R; Somorjai R; Brisson J-R A Monte Carlo Method for Conformational Analysis of Saccharides. Carbohydr. Res 1993, 238, 49–73. [PubMed: 8431939]

(6). Paulsen H; Peters T; Sinnwell V; Lebuhn R; Meyer B Bestimmung der Konformationen von Tri- und Tetrasaccharid-Sequenzen der Core-Struktur von N-Glycoproteinen. Problem der (1–6)-glycosidischen Bindung. Liebigs Ann. Chem 1984, 1984, 951–976.

(7). Jeffrey GA; Taylor R The Application of Molecular Mechanics to the Structures of Carbohydrates. J. Comput. Chem 1980, 1, 99–109.

(8). Taylor R An Empirical Potential for the O-H-O Hydrogen Bond. J. Mol. Struct 1981, 71, 311–325.

(9). Homans SW; Dwek RA; Boyd J; Mahmoudian M; Richards WG; Rademacher TW Conformational Transitions in N-Linked Oligosaccharides. Biochemistry 1986, 25, 6342–6350. [PubMed: 3790526]

(10). Tvaroška I; Pérez S Conformational-Energy Calculations for Oligosaccharides: A Comparison of Methods and a Strategy of Calculation. Carbohydr. Res 1986, 149, 389–410.

(11). Woods RJ; Andrews CW; Bowen JP Molecular Mechanical Investigation of the Properties of Oxocarbenium Ions. 1. Parameter Development. J. Am. Chem. Soc 1992, 114, 850–858.

(12). Woods RJ; Andrews CW; Bowen JP Molecular Mechanical Investigation of the Properties of Oxocarbenium Ions. 2. Application to Glycoside Hydrolysis. J. Am. Chem. Soc 1992, 114, 859–864.

(13). Jimenez-Barbero J; Noble O; Pfeffer C; Perez S Solvent- Specific Energy Surfaces of Carbohydrates: The Mannobiose Case. New J. Chem 1988, 12, 941–946.

(14). Ha SN; Giammona A; Field M; Brady JW A Revised Potential-Energy Surface for Molecular Mechanics Studies of Carbohydrates. Carbohydr. Res 1988, 180, 207–221. [PubMed: 3203342]

(15). Tran V; Buleon A; Imberty A; Perez S Relaxed Potential-Energy Surfaces of Maltose. Biopolymers 1989, 28, 679–690.

(16). French AD; Dowd MK Exploration of Disaccharide Conformations by Molecular Mechanics. J. Mol. Struct.: THEOCHEM 1993, 286, 183–201.

(17). Dowd MK; French AD; Reilly PJ Molecular Mechanics Modeling of a-(1–2)-, a-(1–3)-, and a-(1–6)-Linked Mannosyl Disaccharides withMM3(92). J. Carbohydr. Chem 1995, 14, 589–600.

(18). French AD; Kelterer A-M; Johnson GP; Dowd MK; Cramer CJ HF/6–31G* Energy Surfaces for Disaccharide Analogs. J. Comput. Chem 2001, 22, 65.

(19). Momany FA; Appell M; Willett JL; Schnupf U; Bosma WB DFT Study of alpha- and beta-D-galactopyranose at the B3LYP/6–311++G** Level of Theory. Carbohydr. Res 2006, 341, 525–537. [PubMed: 16414033]

(20). Homans SW; Pastore A; Dwek RA; Rademacher TW Structure and Dynamics in Oligomannose-Type Oligosaccharides. Biochemistry 1987, 26, 6649–6655. [PubMed: 3427033]

(21). Brady JW Molecular Dynamics Simulations of a-D-Glucose. J. Am. Chem. Soc 1986, 108, 8153–8160.

(22). Brady JW Molecular Dynamics Simulations of β-D-Glucopyranose. Carbohydr. Res 1987, 165, 306–312. [PubMed: 3664529]

(23). Homans SW A Molecular Mechanical Force Field for the Conformational Analysis of Oligosaccharides: Comparison of Theoretical and Crystal Structures of Man.alpha.1 −3Man.beta. 1 – 4GlcNAc. Biochemistry 1990, 29, 9110–9118. [PubMed: 2271581]

(24). Edge CJ; Singh UC; Bazzo R; Taylor GL; Dwek RA; Rademacher TW 500-ps Molecular Dynamics in Water of the Man(alpha)1→2Man(alpha) Glycosidic Linkage Present in ASN-Linked Oligomannose-Type Structures on Glycoproteins. Biochemistry 1990, 29, 1971–1974. [PubMed: 2328229]

(25). Woods RJ; Edge CJ; Wormald MR; Dwek RA In Complex Carbohydrates in Drug Research; Alfred Renzon Symposium 36; Bock K, Clausen H, Krogsgaard-Larsen P, Kofod H, Eds.; Munksgaard: Copenhagen, Denmark, 1993.

(26). Kirschner KN; Yongye AB; Tschampel SM; González-Outeiriño J; Daniels CR; Foley BL; Woods RJ GLYCAM06: A Generalizable Biomolecular Force Field. Carbohydrates. J. Comput. Chem 2008, 29, 622–655. [PubMed: 17849372]

(27). Tessier MB; DeMarco ML; Yongye AB; Woods RJ Extension of the GLYCAM06 Biomolecular Force Field to Lipids, Lipid Bilayers and Glycolipids. Mol. Simul 2008, 34, 349–364. [PubMed: 22247593]

(28). Singh A; Tessier MB; Pederson K; Wang X; Venot A; Boons GJ; Prestegard JH; Woods RJ Extension and Validation of the GLYCAM Force Field Parameters for Glycosaminoglycans. Can. J. Chem 2016, 94, 927–935. [PubMed: 28603292]

(29). Wang X; Woods RJ Insights into Furanose Solution Conformations: Beyond the Two-State Model. J. Biomol. NMR 2016, 64, 291–305. [PubMed: 26968894]

(30). Reiling S; Schlenkrich M; Brickmann J Force Field Parameters for Carbohydrates. J. Comput. Chem 1996, 17, 450–468.

(31). Kuttel M; Brady JW; Naidoo KJ Carbohydrate Solution Simulations: Producing a Force Field with Experimentally Consistent Primary Alcohol Rotational Frequencies and Populations. J. Comput. Chem 2002, 23, 1236–1243. [PubMed: 12210149]

(32). Guvench O; Hatcher E; Venable RM; Pastor RW; MacKerell AD CHARMM Additive All-Atom Force Field for Glycosidic Linkages between Hexopyranoses. J. Chem. Theory Comput 2009, 5, 2353–2370. [PubMed: 20161005]

(33). Raman EP; Guvench O; MacKerell AD Jr. CHARMM Additive All-Atom Force Field for Glycosidic Linkages in Carbohydrates Involving Furanoses. J. Phys. Chem. B 2010, 114, 12981–12994. [PubMed: 20845956]

(34). Mallajosyula SS; Guvench O; Hatcher E; MacKerell AD CHARMM Additive All-Atom Force Field for Phosphate and Sulfate Linked to Carbohydrates. J. Chem. Theory Comput 2012, 8, 759–776. [PubMed: 22685386]

(35). Kouwijzer MLCE; van Eijck BP; Kooijman H; Kroon J An Extension of the GROMOS Force Field for Carbohydrates, Resulting in Improvement of the Crystal Structure Determination of aD-Galactose. Acta Crystallogr. Sect. B: Struct. Sci 1995, 51, 209–220.

(36). Ott K-H; Meyer B Parametrization of the GROMOS Force Field for Oligosaccharides and Assessment of Efficiency of Molecular Dynamics Simulations. J. Comput. Chem 1996, 17, 1068–1084.

(37). Spieser SAH; van Kuik JA; Kroon-Batenburg LMJ; Kroon J Improved Carbohydrate Force Field for GROMOS: Ring and Hydroxymethyl Group Conformations and Exo-Anomeric Effect. Carbohydr. Res 1999, 322, 264–273.

(38). Lins RD; Hunenberger PH A New GROMOS Force Field for Hexopyranose-Based Carbohydrates. J. Comput. Chem 2005, 26, 1400–1412. [PubMed: 16035088]

(39). Hansen H; Hünenberger PH A Reoptimized GROMOS Force Field for Hexopyranose-Based Carbohydrates Accounting for the Relative Free Energies of Ring Conformers, Anomers, Epimers, Hydroxymethyl Rotamers, and Glycosidic Linkage Conformers. J. Comput. Chem 2011, 32, 998–1032. [PubMed: 21387332]

(40). Suzuki T; Kajino M; Yanaka S; Zhu T; Yagi H; Satoh T; Yamaguchi T; Kato K Conformational Analysis of a High-Mannose-Type Oligosaccharide Displaying Glucosyl Determinant Recognised by Molecular Chaperones Using NMR-Validated Molecular Dynamics Simulation. ChemBioChem 2017, 18, 396–401. [PubMed: 27995699]

(41). Apweiler R; Hermjakob H; Sharon N On the Frequency of Protein Glycosylation, as Deduced from Analysis of the SWISS-PROT Database. Biochim. Biophys. Acta, Gen. Subj 1999, 1473, 4–8.

(42). Hadden JA; Tessier MB; Fadda E; Woods RJ Calculating Binding Free Energies for Protein-Carbohydrate Complexes. Methods Mol. Biol 2015, 1273, 431–465. [PubMed: 25753724]

(43). Perez S; Tvaroska I Carbohydrate-Protein Interactions: Molecular Modeling Insights. Adv. Carbohyd. Chem. Bi 2014, 71, 9–136.

(44). Fadda E; Woods RJ Molecular Simulations of Carbohydrates and Protein—Carbohydrate Interactions: Motivation, Issues and Prospects. Drug Discovery Today 2010, 15, 596–609. [PubMed: 20594934]

(45). Woods RJ In Reviews in Computational Chemistry, Vol. 9; Lipkowitz KB, Boyd DB, Eds.; VCH Publishers, Inc.: New York, 1996; DOI: 10.1002/9780470125861.ch3.

(46). Weiner PK; Kollman PA AMBER: Assisted Model Building with Energy Refinement. A General Program for Modeling Molecules and Their Interactions. J. Comput. Chem 1981, 2, 287–303.

(47). Imberty A; Gerber S; Tran V; Pérez S Data Bank of Three-Dimensional Structures of Disaccharides, a Tool to Build 3-D Structures of Oligosaccharides. Glycoconjugate J. 1990, 7, 27–54.

(48). Imberty A; Delage M-M; Bourne Y; Cambillau C; Per ez S Data Bank of Three-Dimensional Structures of Disaccharides: Part II, N-Acetyllactosaminic Type N-Glycans. Comparison with the Crystal Structure of a Biantennary Octasaccharide. Glycoconjugate J. 1991, 8, 456–483.

(49). Homans SW; Forster M Application of Restrained Minimization, Simulated Annealing and Molecular Dynamics Simulations for the Conformational Analysis of Oligosaccharides. Glycobiology 1992, 2, 143–151. [PubMed: 1351413]

(50). Jardetzky O Nature of Molecular-Conformations Inferred from High-Resolution NMR. Biochim. Biophys. Ada, Protein Struct 1980, 621, 227–232.

(51). Cumming DA; Carver JP Virtual and Solution Conformations of Oligosaccharides. Biochemistry 1987, 26, 6664–6676. [PubMed: 3427035]

(52). Dowd MK; French AD; Reilly PJ MM3Modeling of Ribose and 2-Deoxyribose Ring Puckering. J. Carbohydr. Chem 2000, 19, 1091–1114.

(53). Weimar T; Woods RJ In NMR Spectroscopy of Glycoconjugates; Jiménez-Barbero J, Peters T, Eds.; Wiley—VCH: Weinheim, Germany, 2003; DOI: 10.1002/352760071X.ch6.

(54). Karplus M Vicinal Proton Coupling in Nuclear Magnetic Resonance. J. Am. Chem. Soc 1963, 85, 2870–2871.

(55). Bose B; Zhao S; Stenutz R; Cloran F; Bondo PB; Bondo G; Hertz B; Carmichael I; Serianni AS Three-Bond C-O-C-C Spin-Coupling Constants in Carbohydrates: Development of a Karplus Relationship. J. Am. Chem. Soc 1998, 120, 11158–11173.

(56). Cano FH; Foces-Foces C; Jiménez-Barbero J; Alemany A; Bernabe M; Martín-Lomas M Experimental Evidence of Deviations from a Karplus-Like Relationship of Vicinal Carbon-Proton Coupling Constants in Some Conformationally Rigid Carbohydrate Derivatives. J. Org. Chem 1987, 52, 3367–3372.

(57). Coxon B Developments in the Karplus Equation as They Relate to the NMR Coupling Constants of Carbohydrates. Adv. Carbohydr. Chem. Biochem 2009, 62, 17–82. [PubMed: 19501704]

(58). Nishida Y; Hori H; Ohrui H; Meguro H 1H NMR Analyses of Rotameric Distribution of C5-C6 Bonds of D-Glucopyranoses in Solution. J. Carbohydr. Chem 1988, 7, 239–250.

(59). Bock K; Duus JØ A Conformational Study of Hydroxymethyl Groups in Carbohydrates Investigated by ^{1}H NMR Spectroscopy. J. Carbohydr. Chem 1994, 13, 513–543.

(60). Zhao H; Pan Q; Zhang W; Carmichael I; Serianni AS DFT and NMR Studies of 2JCOH, 3JHCOH, and 3JCCOH Spin-Couplings in Saccharides: C-O Torsional Bias and H-Bonding in Aqueous Solution. J. Org. Chem 2007, 72, 7071–7082. [PubMed: 17316047]

(61). Yongye AB; Foley BL; Woods RJ On Achieving Experimental Accuracy from Molecular Dynamics Simulations of Flexible Molecules: Aqueous Glycerol. J. Phys. Chem. A 2008, 112, 2634–2639. [PubMed: 18311953]

(62). Gonzalez-Outeiriño J; Kirschner KN; Thobhani S; Woods RJ Reconciling Solvent Effects on Rotamer Populations in Carbohydrates: A Joint MD and NMR Analysis. Can. J. Chem 2006, 84, 569–579. [PubMed: 25544777]

(63). González-Outeiriño J; Kadirvelraj R; Woods RJ Structural Elucidation of Type III Group B *Streptococcus* Capsular Polysaccharide Using Molecular Dynamics Simulations: The Role of Sialic Acid. Carbohydr. Res 2005, 340, 1007–1018. [PubMed: 15780265]

(64). Sattelle BM; Shakeri J; Almond A Does Microsecond Sugar Ring Flexing Encode 3D-Shape and Bioactivity in the Heparanome? Biomacromolecules 2013, 14, 1149–1159. [PubMed: 23439078]

(65). Yongye AB; Gonzales-Outeirño J; Glushka J; Schultheis V; Woods RJ The Conformational Properties of Methyl α-(2,8)-di/trisialosides and Their N-acyl Analogs: Implications for Anti-Neisseria meningitidis B Vaccine Design. Biochemistry 2008, 47, 12493–12514. [PubMed: 18954144]

(66). Bock K; Duus JO; Refn S Conformational Equilibria of 4-Thiomaltose and Nitrogen Analogues of Maltose in Aqueous Solutions. Carbohydr. Res 1994, 253, 51–67. [PubMed: 8156558]

(67). Pople JA; Schneider WG; Bernstein HJ High-Resolution Nuclear Magnetic Resonance; McGraw-Hill: New York, 1959.

(68). Sattelle BM; Hansen SU; Gardiner J; Almond A Free Energy Landscapes of Iduronic Acid and Related Monosaccharides. J. Am. Chem. Soc 2010, 132, 13132–13134. [PubMed: 20809637]

(69). Gonzalez-Outeiriño J; Kadirvelraj R; Woods RJ Structural Elucidation of Type III Group B *Streptococcus* Capsular Polysaccharide Using Molecular Dynamics Simulations: The Role of Sialic Acid. Carbohydr. Res 2005, 340, 1007–1018. [PubMed: 15780265]

(70). Tian F; Al-Hashimi HM; Craighead JL; Prestegard JH Conformational Analysis of a Flexible Oligosaccharide Using Residual Dipolar Couplings. J. Am. Chem. Soc 2001, 123, 485–492. [PubMed: 11456551]

(71). Bell NGA; Rigg G; Masters S; Bella J; Uhrin D Detecting Low-Level Flexibility Using Residual Dipolar Couplings: A Study of the Conformation of Cellobiose. Phys. Chem. Chem. Phys 2013, 15, 18223–18234. [PubMed: 24064673]

(72). Battistel MD; Azurmendi HF; Yu B; Freedberg DI NMR of Glycans: Shedding New Light on Old Problems. Prog. Nucl Magn. Reson. Spectrosc 2014, 79, 48–68. [PubMed: 24815364]

(73). Esteban-Martin S; Fenwick RB; Salvatella X Synergistic Use of NMR and MD Simulations to Study the Structural Heterogeneity of Proteins. Wiley Interdiscip. Rev. Comput. Mol. Sci 2012, 2, 466–478.

(74). Tjandra N; Bax A Direct Measurement of Distances and Angles in Biomolecules by NMR in a Dilute Liquid Crystalline Medium. Science 1997, 278, 1111–1114. [PubMed: 9353189]

(75). Tolman JR; Flanagan JM; Kennedy MA; Prestegard JH Nuclear Magnetic Dipole Interactions in Field Oriented Proteins: Information for Structure Determination in Solution. Proc. Natl. Acad. Sci. U. S. A 1995, 92, 9279–9283. [PubMed: 7568117]

(76). Freedberg DI An Alternative Method for Pucker Determination in Carbohydrates from Residual Dipolar Couplings: A Solution NMR Study of the Fructofuranosyl Ring of Sucrose. J. Am. Chem. Soc 2002, 124, 2358–2362. [PubMed: 11878992]

(77). Venable R; Delaglio F; Norris SE; Freedberg DI The Utility of Residual Dipolar Couplings in Detecting Motion in Carbohydrates: Application to Sucrose. Carbohydr. Res 2005, 340, 863–874. [PubMed: 15780252]

(78). Pham TN; Hinchley SL; Rankin DW; Liptaj T; Uhrin D Determination of Sugar Structures in Solution from Residual Dipolar Coupling Constants: Methodology and Application to Methyl Beta-D-Xylopyranoside. J. Am. Chem. Soc 2004, 126, 13100–13110. [PubMed: 15469309]

(79). Jain NU; Noble S; Prestegard JH Structural Characterization of a Mannose-Binding Protein-Trimannoside Complex Using Residual Dipolar Couplings. J. Mol. Biol 2003, 328, 451–462. [PubMed: 12691753]

(80). Zhuang T; Leffler H; Prestegard JH Enhancement of Bound-State Residual Dipolar Couplings: Conformational Analysis of Lactose Bound to Galectin-3. Protein Sci. 2006, 15, 1780–1790. [PubMed: 16751604]

(81). Mackeen MM; Almond A; Deschamps M; Cumpstey I; Fairbanks AJ; Tsang C; Rudd PM; Butters TD; Dwek RA; Wormald MR The Conformational Properties of the Glc(3)Man Unit Suggest Conformational Biasing within the Chaperone-Assisted Glycoprotein Folding Pathway. J. Mol. Biol 2009, 387, 335–347. [PubMed: 19356590]

(82). Jin L; Hricovini M; Deakin JA; Lyon M; Uhrin D Residual Dipolar Coupling Investigation of a Heparin Tetrasaccharide Confirms the Limited Effect of Flexibility of the Iduronic Acid on the Molecular Shape of Heparin. Glycobiology 2009, 19, 1185–1196. [PubMed: 19648354]

(83). Ganguly S; Xia J; Margulis C; Stanwyck L; Bush CA Measuring the Magnitude of Internal Motion in a Complex Hexasaccharide. Biopolymers 2011, 95, 39–50. [PubMed: 20683925]

(84). Xia J; Case DA Sucrose in Aqueous Solution Revisited, Part 1: Molecular Dynamics Simulations and Direct and Indirect Dipolar Coupling Analysis. Biopolymers 2012, 97, 276–288. [PubMed: 22189655]

(85). Yu F; Wolff JJ; Amster IJ; Prestegard JH Conformational Preferences of Chondroitin Sulfate Oligomers Using Partially Oriented NMR Spectroscopy of C-13-labeled Acetyl Groups. J. Am. Chem. Soc 2007, 129, 13288–13297. [PubMed: 17924631]

(86). Sawen E; Stevensson B; Ostervall J; Maliniak A; Widmalm G Molecular Conformations in the Pentasaccharide LNF-1 Derived from NMR Spectroscopy and Molecular Dynamics Simulations. J. Phys. Chem. B 2011, 115, 7109–7121. [PubMed: 21545157]

(87). Almond A; Bunkenborg J; Franch T; Gotfredsen CH; Duus JO Comparison of Aqueous Molecular Dynamics with NMR Relaxation and Residual Dipolar Couplings Favors Internal Motion in a Mannose Oligosaccharide. J. Am. Chem. Soc 2001, 123, 4792–4802. [PubMed: 11457289]

(88). Martin-Pastor M; Canales A; Corzana F; Asensio JL; Jimenez-Barbero J Limited Flexibility of Lactose Detected from Residual Dipolar Couplings Using Molecular Dynamics Simulations and Steric Alignment Methods. J. Am. Chem. Soc 2005, 127, 3589–3595. [PubMed: 15755180]

(89). Sanderson PN; Huckerby TN; Nieduszynski IA Conformational Equilibria of Alpha-L-Iduronate Residues in Disaccharides Derived from Heparin. Biochem. J 1987, 243, 175–181. [PubMed: 3038077]

(90). Ferro DR; Provasoli A; Ragazzi M; Casu B; Torri G; Bossennec V; Perly B; Sinay P; Petitou M; Choay J Conformer Populations of L-Iduronic Acid Residues in Glycosaminoglycan Sequences. Carbohydr. Res 1990, 195, 157–167. [PubMed: 2331699]

(91). Torri G; Casu B; Gatti G; Petitou M; Choay J; Jacquinet JC; Sinay P Mono- and Bidimensional 500MHz 1H-NMRSpectra of a Synthetic Pentasaccharide Corresponding to the Binding Sequence of Heparin to Antithrombin-Iii: Evidence for Conformational Peculiarity of the Sulfated Iduronate Residue. Biochem. Biophys. Res. Commun 1985, 128, 134–140. [PubMed: 3985961]

(92). Casu B; Petitou M; Provasoli M; Sinay P Conformational Flexibility: A New Concept for Explaining Binding and Biological Properties of Iduronic Acid-Containing Glycosaminoglycans. Trends Biochem. Sci 1988, 13, 221–225. [PubMed: 3076283]

(93). Hsieh PH; Thieker DF; Guerrini M; Woods RJ; Liu J Uncovering the Relationship between Sulphation Patterns and Conformation of Iduronic Acid in Heparan Sulphate. Sci. Rep 2016, 6, No. 29602. [PubMed: 27412370]

(94). Lipari G; Szabo A Model-Free Approach to the Interpretation of Nuclear Magnetic Resonance Relaxation in Macromolecules. 1. Theory and Range of Validity. J. Am. Chem. Soc 1982, 104, 4546–4558.

(95). Brisson J-R; Carver JP Solution Conformation of a D(1–3)- and aD(1–6)-Linked Oligomannosides Using Proton Nuclear Magnetic Resonance. Biochemistry 1983, 22, 1362–1368. [PubMed: 6838858]

(96). Sheikh MO; Thieker D; Chalmers G; Schafer CM; Ishihara M; Azadi P; Woods RJ; Glushka JN; Bendiak B; Prestegard JH; et al. O2 Sensing Associated Glycosylation Exposes the F-Box Combining Site of the Dictyostelium Skp1 Subunit in E3 Ubiquitin Ligases. J. Biol. Chem 2017, 292, 18897–18915. [PubMed: 28928219]

(97). Woods RJ; Pathiaseril A; Wormald MR; Edge CJ; Dwek RA The High Degree of Internal Flexibility Observed for an Oligomannose Oligosaccharide Does Not Alter the Overall Topology of the Molecule. Eur. J. Biochem 1998, 258, 372–386. [PubMed: 9874202]

(98). Wormald MR; Edge CJ The Systematic Use of Negative Nuclear Overhauser Constraints in the Determination of Oligosaccharide Conformations: Application to Sialyl-Lewis X. Carbohydr. Res 1993, 246, 337–344. [PubMed: 8103705]

(99). Bush CA; Yan Z-Y; Rao BNN Conformational Energy Calculations and Proton Nuclear Overhauser Enhancements Reveal a Unique Conformation for Blood Group A Oligosaccharides. J. Am. Chem. Soc 1986, 108, 6168–6173.

(100). Moseley HN; Curto EV; Krishna N R Complete Relaxation and Conformational Exchange Matrix (CORCEMA) Analysis of NOESY Spectra of Interacting Systems; Two-Dimensional Transferred NOESY. J. Magn. Reson., Ser. B 1995, 108, 243–261; Correction. 1996, 110, 321 DOI: 10.1006/jmrb.1996.0051. [PubMed: 7670757]

(101). Landstrom J; Widmalm G Glycan Flexibility: Insights into Nanosecond Dynamics from a Microsecond Molecular Dynamics Simulation Explaining an Unusual Nuclear Overhauser Effect. Carbohydr. Res 2010, 345, 330–333. [PubMed: 19962132]

(102). Lipari G; Szabo A Model-Free Approach to the Interpretation of Nuclear Magnetic Resonance Relaxation in Macromolecules. 2. Analysis of Experimental Results. J. Am. Chem. Soc 1982, 104, 4559–4570.

(103). Chalmers G; Glushka JN; Foley BL; Woods RJ; Prestegard JH Direct Noe Simulation from Long MD Trajectories. J. Magn. Reso.n 2016, 265, 1–9.

(104). Mayer M; Meyer B Group Epitope Mapping by Saturation Transfer Difference NMR to Identify Segments of a Ligand in Direct Contact with a Protein Receptor. J. Am. Chem. Soc 2001, 123, 6108–6117. [PubMed: 11414845]

(105). Meyer B; Peters T NMR Spectroscopy Techniques for Screening and Identifying Ligand Binding to Protein Receptors. Angew. Chem., Int. Ed 2003, 42, 864–890.

(106). Haselhorst T; Lamerz AC; Itzstein M Saturation Transfer Difference NMR Spectroscopy as a Technique to Investigate ProteinCarbohydrate Interactions in Solution. Method. Mol. Biol 2009, 534, 375–386.

(107). Hemmi H NMR Analysis of Carbohydrate-Binding Interactions in Solution: An Approach Using Analysis of Saturation Transfer Difference NMR Spectroscopy. Methods Mol. Biol 2014, 1200, 501–509. [PubMed: 25117260]

(108). Krishna NR; Jayalakshmi V Quantitative Analysis of STD-NMR Spectra of Reversibly Forming Ligand-Receptor Complexes. Top. Curr. Chem 2007, 273, 15–54.

(109). Enriquez-Navas PM; Guzzi C; Munoz-Garcia JC; Nieto PM; Angulo J Structures of Glycans Bound to Receptors from Saturation Transfer Difference (Std) NMR Spectroscopy: Quantitative Analysis by Using CORCEMA-St. Methods Mol Biol. 2015, 1273, 475–487. [PubMed: 25753726]

(110). Lak P; Makeneni S; Woods RJ; Lowary TL Specificity of Furanoside-Protein Recognition through Antibody Engineering and Molecular Modeling. Chem. - Eur. J 2015, 21, 1138–1148. [PubMed: 25413161]

(111). Tessier MB; Grant OC; Heimburg-Molinaro J; Smith D; Jadey S; Gulick AM; Glushka J; Deutscher SL; Rittenhouse-Olson K; Woods RJ Computational Screening of the Human TF-Glycome Provides a Structural Definition for the Specificity of Anti-Tumor Antibody JAA-F11. PLoS One 2013, 8, e54874. [PubMed: 23365681]

(112). Johnson MA; Cartmell J; Weisser NE; Woods RJ; Bundle DR Molecular Recognition of Candida albicans (1→2)-β-Mannan Oligosaccharides by a Protective Monoclonal Antibody Reveals the Immunodominance of Internal Saccharide Residues. J. Biol Chem 2012, 287, 18078–18090. [PubMed: 22493450]

(113). Ponader D; Maffre P; Aretz J; Pussak D; Ninnemann NM; Schmidt S; Seeberger PH; Rademacher C; Nienhaus GU; Hartmann L Carbohydrate-Lectin Recognition of Sequence-Defined Heteromultivalent Glycooligomers. J. Am. Chem. Soc 2014, 136, 2008–2016. [PubMed: 24417254]

(114). Enríquez-Navas PM; Marradi M; Padro D; Angulo J; Penadés S A Solution NMR Study of the Interactions of Oligomanno-sides and the Anti-HIV-1 2G12 Antibody Reveals Distinct Binding Modes for Branched Ligands*. Chem. - Eur. J 2011, 17, 1547–1560. [PubMed: 21268157]

(115). Pederson K; Mitchell DA; Prestegard JH Structural Characterization of the Dc-Sign-Lewis(X) Complex. Biochemistry 2014, 53, 5700–5709. [PubMed: 25121780]

(116). Vliegenhart JFG; Woods RJ NMR Spectroscopy and Computer Modeling of Carbohydrates: Recent Advances; American Chemical Society: Washington, DC, 2006; DOI: 10.1021/bk-2006-0930.

(117). Sattelle BM; Bose-Basu B; Tessier M; Woods RJ; Serianni AS; Almond A Dependence of Pyranose Ring Puckering on Anomeric Configuration: Methyl Idopyranosides. J. Phys. Chem. B 2012, 116, 6380–6386. [PubMed: 22577942]

(118). Dorn M; Barbachan e Silva M; Buriol LS; Lamb LC Three-Dimensional Protein Structure Prediction: Methods and Computational Strategies. Comput. Biol. Chem 2014, 53B, 251–276.

(119). Zwanzig R; Szabo A; Bagchi B Levinthal's Paradox. Proc. Natl. Acad. Sci U. S. A 1992, S9, 20–22. [PubMed: 1729690]

(120). Levinthal C Are There Pathways for Protein Folding. J. Chim. Phys. Phys.-Chim. Biol 1968, 65, 44–45.

(121). Rao VSR; Qasba PK; Balaji PV; Chandrasekaran R Conformation of Carbohydrates; Harwood Academic Publishers; 1998; p 359.

(122). Kirschner KN; Woods RJ Solvent Interactions Determine Carbohydrate Conformation. Proc. Natl. Acad. Sci. U. S. A 2001, 98, 10541–10545. [PubMed: 11526221]

(123). Wolfe S; Myung-Hwan W; Mitchell DJ On the Magnitudes and Origins of the "Anomeric Effects", "Exo-Anomeric Effects", "Reverse Anomeric Effects", and C-X and C-Y Bond Lengths in XCH2YH Molecules. Carbohydr. Res 1979, 69, 1–26.

(124). Booth H; Khedhair KA *endo*-Anomeric and *exo*-Anomeric Effects in 2-Substituted Tetrahydropyrans. J. Chem. Soc., Chem. Commun 1985, 467–468.

(125). Booth H; Grindley TB; Khedhair KA The Anomeric and exo-Anomeric Effects in 2-Methoxytetrahydropyran. J. Chem. Soc., Chem. Commun 1982, 0, 1047–1048.

(126). Tvaroska I; Carver JP Ab Initio Molecular Orbital Calculation of Carbohydrate Model Compounds 0.5. Anomeric, Exo-Anomeric, and Reverse Anomeric Effects in C-, N-, and S-Glycosyl Compounds. J. Phys. Chem 1996, 100, 11305–11313.

(127). Peric-Hassler L; Hansen HS; Baron R; Hunenberger PH Conformational Properties of Glucose-Based Disaccharides Investigated Using Molecular Dynamics Simulations with Local Elevation Umbrella Sampling. Carbohydr. Res 2010, 345, 1781–1801. [PubMed: 20576257]

(128). Salisburg AM; Deline AL; Lexa KW; Shields GC; Kirschner KN Ramachandran-Type Plots for Glycosidic Linkages: Examples from Molecular Dynamic Simulations Using the Glycam06 Force Field. J. Comput. Chem 2009, 30, 910–921. [PubMed: 18785152]

(129). Imberty A; Mikros E; Koca J; Mollicone R; Oriol R; Perez S Computer Simulation of Histo-Blood Group Oligosaccharides: Energy Maps of All Constituting Disaccharides and Potential Energy Surfaces of 14ABH and Lewis Carbohydrate Antigens. Glycoconjugate J. 1995, 12, 331–349.

(130). Stortz CA; Johnson GP; French AD; Csonka GI Comparison of Different Force Fields for the Study of Disaccharides. Carbohydr. Res 2009, 344, 2217–2228. [PubMed: 19758584]

(131). Schnupf U; Willett JL; Bosma WB; Momany FA DFT Studies of the Disaccharide, Alpha-Maltose: Relaxed Isopotential Maps. Carbohydr. Res 2007, 342, 2270–2285. [PubMed: 17669381]

(132). Topin J; Lelimousin M; Arnaud J; Audfray A; Perez S; Varrot A; Imberty A The Hidden Conformation of Lewis X, a Human Histo-Blood Group Antigen, Is a Determinant for Recognition by Pathogen Lectins. ACS Chem. Biol 2016, 11, 2011–2020. [PubMed: 27198630]

(133). Jo S; Qi Y; Im W Preferred Conformations of N-Glycan Core Pentasaccharide in Solution and in Glycoproteins. Glycobiology 2016, 26, 19–29. [PubMed: 26405106]

(134). Hadden J; French AD; Woods R Effect of Microfibril Twisting on Theoretical Powder Diffraction Patterns of Cellulose Iβ. Cellulose 2014, 21, 879–884. [PubMed: 24729665]

(135). Hadden JA; French AD; Woods RJ Unraveling Cellulose Microfibrils: A Twisted Tale. Biopolymers 2013, 99, 746–756. [PubMed: 23681971]

(136). Matthews JF; Beckham GT; Bergenstråhle-Wohlert M; Brady JW; Himmel ME; Crowley MF Comparison of Cellulose Iβ Simulations with Three Carbohydrate Force Fields. J. Chem. Theory Comput 2012, 8, 735–748. [PubMed: 26596620]

(137). Nishida Y; Ohrui H; Meguro H 1H-NMR Studies of (6R)- and (6S)-Deuterated D-Hexoses: Assignment of the Preferred Rotamers About C5-C6 Bond of D-Glucose and D-Galactose Derivatives in Solutions. Tetrahedron Lett. 1984, 25, 1575–1578.

(138). Ohrui H; Nishida Y; Watanabe M; Hori H; Meguro H 1H- NMR Studies of (6R)- and (6S)-Deuterated (1–6)-Linked Disaccharides: Assignment of the Preferred Rotamers About C5-C6 Bond of (1–6)-Disaccharides in Solution. Tetrahedron Lett. 1985, 26, 3251–3254.

(139). Hori H; Nishida Y; Ohrui H; Meguro H; Uzawa J Conformational Analyses of a and B (1–6) Mannodisaccharides by Deuterium Substitution Effect on Relaxation Rate and Noe. Tetrahedron Lett. 1988, 29, 4457–4460.

(140). Tvaroska I; Carver JP Ab Initio Molecular Orbital Calculation of Carbohydrate Model Compounds. 6. The Gauche Effect and Conformations of the Hydroxymethyl Groups. J. Phys. Chem. B 1997, 101, 2992–2999.

(141). Wolfe S Gauche Effect. Some Stereochemical Consequences of Adjacent Electron Pairs and Polar Bonds. Acc. Chem. Res 1972, 5, 102–111.

(142). Wiberg KB; Murcko MA; Laidig KE; MacDougall PJ Origin of the “Gauche Effect” in Substituted Ethanes and Ethenes. J. Phys. Chem 1990, 94, 6956–6959.

(143). Rockwell GD; Grindley BT Effect of Solvation on the Rotation of Hydroxymethyl Groups in Carbohydrates. J. Am. Chem. Soc 1998, 120, 10953–10963.

(144). Kamiya Y; Yanagi K; Kitajima T; Yamaguchi T; Chiba Y; Kato K Application of Metabolic 13C Labeling in Conjunction with High-Field Nuclear Magnetic Resonance Spectroscopy for Comparative Conformational Analysis of High Mannose-Type Oligosaccharides. Biomolecules 2013, 3, 108–123. [PubMed: 24970159]

(145). Thieker DF; Hadden JA; Schulten K; Woods RJ 3D Implementation of the Symbol Nomenclature for Graphical Representation of Glycans. Glycobiology 2016, 26, 786–787. [PubMed: 27514939]

(146). Varki A; Cummings RD; Aebi M; Packer NH; Seeberger PH; Esko JD; Stanley P; Hart G; Darvill A; Kinoshita T; et al. Symbol Nomenclature for Graphical Representations of Glycans. Glycobiology 2015, 25, 1323–1324. [PubMed: 26543186]

(147). Humphrey W; Dalke A; Schulten K VMD - Visual Molecular Dynamics. J. Mol. Graphics 1996, 14, 33–38.

(148). Lee G; Nowak W; Jaroniec J; Zhang Q; Marszalek PE Molecular Dynamics Simulations of Forced Conformational Transitions in 1,6-Linked Polysaccharides. Biophys. J 2004, 87, 1456–1465. [PubMed: 15345528]

(149). Perlin AS; Casu B; Sanderson GR; Tse J Methyl Alpha and Beta-D-Idopyranosiduronic Acids Synthesis and Conformational-Analysis. Carbohydr. Res 1972, 21, 123–132.

(150). Sattelle BM; Almond A Is N-acetyl-D-Glucosamine a Rigid 4C1-Chair? Glycobiology 2011, 21, 1651–1662. [PubMed: 21807769]

(151). Hatcher E; Guvench O; MacKerell AD Jr. CHARMM Additive All-Atom Force Field for Aldopentofuranoses, Methyl-aldopentofuranosides, and Fructofuranose. J. Phys. Chem. B 2009, 113, 12466–12476. [PubMed: 19694450]

(152). Queiroz IN; Wang X; Glushka JN; Santos GR; Valente AP; Prestegard JH; Woods RJ; Mourao PA; Pomin VH Impact of Sulfation Pattern on the Conformation and Dynamics of Sulfated Fucan Oligosaccharides as Revealed by NMR and MD. Glycobiology 2015, 25, 535–547. [PubMed: 25527427]

(153). Remko M; von der Lieth CW Gas-Phase and Solution Conformations of the alpha-L-iduronic Acid Structural Unit of Heparin. J. Chem. Inf. Model 2006, 46, 1194–1200. [PubMed: 16711739]

(154). Battistel MD; Shangold M; Trinh L; Shiloach J; Freedberg DI Evidence for Helical Structure in a Tetramer of Alpha2–8 Sialic Acid: Unveiling a Structural Antigen. J. Am. Chem. Soc 2012, 134, 10717–10720. [PubMed: 22703338]

(155). Muhlenhoff M; Eckhardt M; Gerardy-Schahn R Polysialic Acid: Three-Dimensional Structure, Biosynthesis and Function. Curr. Opin. Struct. Biol 1998, 8, 558–564. [PubMed: 9818258]

(156). Baumann H; Brisson J-R; Michon F; Pon R; Jennings HJ Comparison of the Conformation of the Epitope of a(2–8) Polysialic Acid with Its Reduced and *N*-Acyl Derivatives. Biochemistry 1993, 32, 4007–4013. [PubMed: 7682439]

(157). Brisson J-R; Baumann H; Imberty A; Pérez S; Jennings HJ Helical Epitope of the Group B Meningococcal a(2–8)-Linked Sialic Acid Polysaccharide. Biochemistry 1992, 31, 4996–5004. [PubMed: 1376145]

(158). Azurmendi HF; Battistel MD; Zarb J; Lichaa F; Negrete Virgen A; Shiloach J; Freedberg DI The Beta-Reducing End in Alpha(2–8)-Polysialic Acid Constitutes a Unique Structural Motif. Glycobiology 2017, 27, 900–911. [PubMed: 28369425]

(159). Azurmendi HF; Vionnet J; Wrightson L; Trinh L; Shiloach J; Freedberg DI Extracellular Structure of Polysialic Acid Explored by on Cell Solution NMR Proc. Natl. Acad. Sci U. S. A 2007, 104, 11557–11561. [PubMed: 17609375]

(160). Evans SV; Sigurskjold BW; Jennings HJ; Brisson J-R; To R; Tse WC; Altman E; Frosch M; Weisgerber C; Kratzin HD; et al. Evidence for the Extended Helical Nature of Polysaccharide Epitopes. The 2.8 Å Resolution Structure and Thermodynamics of Ligand Binding of an Antigen Binding Fragment Specific for a-(2–8)-Polysialic Acid. Biochemistry 1995, 34, 6737–6744. [PubMed: 7538787]

(161). Hayrinen J; Haseley S; Talaga P; Muhlenhoff M; Finne J; Vliegenthart JF High Affinity Binding of Long-Chain Polysialic Acid to Antibody, and Modulation by Divalent Cations and Polyamines. Mol. Immunol 2002, 39, 399–411. [PubMed: 12413691]

(162). Li H; Ngo V; Da Silva MC; Salahub DR; Callahan K; Roux B; Noskov SY Representation of Ion-Protein Interactions Using the Drude Polarizable Force-Field. J. Phys. Chem. B 2015, 119, 9401–9416. [PubMed: 25578354]

(163). Yoo J; Wilson J; Aksimentiev A Improved Model of Hydrated Calcium Ion for Molecular Dynamics Simulations Using Classical Biomolecular Force Fields. Biopolymers 2016, 105, 752–763. [PubMed: 27144470]

(164). Ibragimova GT; Wade R C. Importance of Explicit Salt Ions for Protein Stability in Molecular Dynamics Simulation. Biophys. J 1998, 74, 2906–2911. [PubMed: 9635744]

(165). Shimoda Y; Kitajima K; Inoue S; Inoue Y Calcium-Ion Binding of 3 Different Types of Oligo/Polysialic Acids as Studied by Equilibrium Dialysis and Circular Dichroic Methods. Biochemistry 1994, 33, 1202–1208. [PubMed: 8110751]

(166). Xin YJ; Bligh MW; Kinsela AS; Wang Y; Waite TD Calcium-Mediated Polysaccharide Gel Formation and Breakage: Impact on Membrane Foulant Hydraulic Properties. J. Membr. Sci 2015, 475, 395–405.

(167). Jaques LW; Brown EB; Barrett JM; Brey WS Jr.; Weltner W Jr. Sialic Acid: A Calcium-Binding Carbohydrate. J. Biol. Chem 1977, 252, 4533–4538 (http://www.jbc.org/content/252/13/4533.full.pdf). [PubMed: 873904]

(168). Yang L; Su Y; Xu Y; Wang Z; Guo Z; Weng S; Yan C; Zhang S; Wu J Interactions between Metal Ions and Carbohydrates. Coordination Behavior of Neutral Erythritol to Ca(II) and Lanthanide Ions. Inorg. Chem 2003, 42, 5844–5856. [PubMed: 12971752]

(169). Gerlits OO; Coates L; Woods RJ; Kovalevsky A Mannobiose Binding Induces Changes in Hydrogen Bonding and Protonation States ofAcidic Residues in Concanavalin A as Revealed by Neutron Crystallography. Biochemistry 2017, 56, 4747–4750. [PubMed: 28846383]

(170). Fadda E; Woods RJ On the Role of Water Models in Quantifying the Binding Free Energy of Highly Conserved Water Molecules in Proteins: The Case of Concanavalin A. J. Chem. Theory Comput 2011, 7, 3391–3398. [PubMed: 26598169]

(171). Kadirvelraj R; Foley BL; Dyekjær JD; Woods R J. Involvement of Water in Carbohydrate-Protein Binding: Concanavalin A Revisited. J. Am. Chem. Soc 2008, 130, 16933–16942. [PubMed: 19053475]

(172). Sakakura M; Oo-Puthinan S; Moriyama C; Kimura T; Moriya J; Irimura T; Shimada I Carbohydrate Binding Mechanism of the Macrophage Galactose-type C-type Lectin 1 Revealed by Saturation Transfer Experiments. J. Biol. Chem 2008, 283, 33665–33673. [PubMed: 18790731]

(173). McGreal EP; Miller JL; Gordon S Ligand Recognition by Antigen-Presenting Cell C-type Lectin Receptors. Curr. Opin. Immunol 2005, 17, 18–24. [PubMed: 15653305]

(174). Cambi A; Figdor CG Levels of Complexity in Pathogen Recognition by C-type Lectins. Curr. Opin. Immunol 2005, 17, 345–351. [PubMed: 15950451]

(175). Kolatkar AR; Weis WI Structural Basis of Galactose Recognition by C-Type Animal Lectins. J. Biol. Chem 1996, 271, 6679–6685. [PubMed: 8636086]

(176). Drickamer K Engineering Galactose-Binding Activity into a C-Type Mannose-Binding Protein. Nature 1992, 360, 183–186. [PubMed: 1279438]

(177). Weis WI; Drickamer K; Hendrickson WA Structure of a C-Type Mannose-Binding Protein Complexed with an Oligosaccharide. Nature 1992, 360, 127–134. [PubMed: 1436090]

(178). Nodet G; Poggi L; Abergel D; Gourmala C; Dong D; Zhang Y; Mallet JM; Bodenhausen G Weak Calcium-Mediated Interactions between Lewis X-Related Trisaccharides Studied by NMR Measurements of Residual Dipolar Couplings. J. Am. Chem. Soc 2007, 129, 9080–9085. [PubMed: 17608422]

(179). Behr JP; Lehn JM Stability-Constants for Complexation of Alkali and Alkaline-Earth Cations by N-Acetyl-Neuraminic Acid. FEBS Lett. 1972, 22, 178–180. [PubMed: 11946590]

(180). Anderson CM Hypothesis Revisited: Cystic Fibrosis: A Disturbance of Water and Electrolyte Movement in Exocrine Secretory Tissue Associated with Altered Prostaglandin (PGE2) Metabolism? J. Pediatr. Gastroenterol. Nutr 1984, 3, 15–22. [PubMed: 6582248]

(181). Waller RL; Brattin WJ; Dearborn DG Cytosolic Free Calcium Concentration and Intracellular Calcium Distribution in Lymphocytes from Cystic Fibrosis Patients. Life Sci. 1984, 35, 775–781. [PubMed: 6472057]

(182). Ponasenko AV; Kutikhin AG; Khutornaya MV; Rutkovskaya NV; Kondyukova NV; Odarenko YN; Kazachek YV; Tsepokina AV; Barbarash LS; Yuzhalin AE Inherited Variation in Cytokine,

Acute Phase Response, and Calcium Metabolism Genes Affects Susceptibility to Infective Endocarditis. Mediators Inflammation 2017, 2017, No. 7962546.

(183). Kuttel MM; Cescutti P; Distefano M; Rizzo R Fluorescence and NMR Spectroscopy Together with Molecular Simulations Reveal Amphiphilic Characteristics of a Burkholderia Biofilm Exopolysaccharide. J. Biol. Chem 2017, 292, 11034–11042. [PubMed: 28468829]

(184). Seviour T; Malde AK; Kjelleberg S; Yuan Z; Mark AE Molecular Dynamics Unlocks Atomic Level Self-Assembly of the Exopolysaccharide Matrix of Water-Treatment Granular Biofilms. Biomacromolecules 2012, 13, 1965–1972. [PubMed: 22587230]

(185). Spillmann D; Burger MM Carbohydrate-Carbohydrate Interactions in Adhesion. J. Cell. Biochem 1996, 61, 562–568. [PubMed: 8806079]

(186). Bucior I; Burger MM Carbohydrate-Carbohydrate Interactions in Cell Recognition. Curr. Opin. Struct. Biol 2004, 14, 631–637. [PubMed: 15465325]

(187). Reynolds AJ; Haines AH; Russell DA Gold Glyconanoparticles for Mimics and Measurement of Metal IonMediated Carbohydrate-Carbohydrate Interactions. Langmuir 2006, 22, 1156–1163. [PubMed: 16430279]

(188). Carvalho de Souza A; Kamerling JP Analysis of Carbohydrate-Carbohydrate Interactions Using Gold Glyconanoparticles and Oligosaccharide Self-Assembling Monolayers. Methods Enzymol 2006, 417, 221–243. [PubMed: 17132508]

(189). Santos JI; Carvalho de Souza A; Canada FJ; Martin-Santamaria S; Kamerling JP; Jimenez-Barbero J Assessing Carbohydrate-Carbohydrate Interactions by NMR Spectroscopy: The Trisaccharide Epitope from the Marine Sponge Microciona Prolifera. Chem Bio Chem 2009, 10, 511–519.

(190). Lorenz B; Alvarez de Cienfuegos L; Oelkers M; Kriemen E; Brand C; Stephan M; Sunnick E; Yuksel D; Kalsani V; Kumar K; et al. Model System for Cell Adhesion Mediated by Weak Carbohydrate-Carbohydrate Interactions. J. Am. Chem. Soc 2012, 134, 3326–3329. [PubMed: 22296574]

(191). Bavireddi H; Bharate P; Kikkeri R Probing CarbohydrateCarbohydrate Interactions by Photoswitchable Supramolecular Glyco-clusters. Chem. Commun 2013, 49, 3988–3990.

(192). Lai CH; Hutter J; Hsu CW; Tanaka H; Varela-Aramburu S; De Cola L; Lepenies B; Seeberger PH Analysis of Carbohydrate-Carbohydrate Interactions Using Sugar-Functionalized Silicon Nanoparticles for Cell Imaging. Nano Lett. 2016, 16, 807–811. [PubMed: 26652315]

(193). de la Fuente JM; Penades S Understanding CarbohydrateCarbohydrate Interactions by Means of Glyconanotechnology. Glycoconjugate J. 2004, 21, 149–163.

(194). Bucior I; Scheuring S; Engel A; Burger MM Carbohydrate-Carbohydrate Interaction Provides Adhesion Force and Specificity for Cellular Recognition. J. Cell Biol 2004, 165, 529–537. [PubMed: 15148309]

(195). Sauter J; Grafmuller A Predicting the Chemical Potential and Osmotic Pressure of Polysaccharide Solutions by Molecular Simulations. J. Chem. Theory Comput 2016, 12, 4375–4384. [PubMed: 27529356]

(196). Lay WK; Miller MS; Elcock AH Optimizing Solute- Solute Interactions in the GLYCAM06 and CHARMM36 Carbohydrate Force Fields Using Osmotic Pressure Measurements. J. Chem. Theory Comput 2016, 12, 1401–1407. [PubMed: 26967542]

(197). Jorgensen WL; Chandrasekhar J; Madura JD; Impey RW; Klein ML Comparison of Simple Potential Functions for Simulating Liquid Water. J. Chem. Phys 1983, 79, 926–935.

(198). Mahoney MW; Jorgensen WL A Five-Site Model for Liquid Water and the Reproduction of the Density Anomaly by Rigid, Nonpolarizable Potential Functions. J. Chem. Phys 2000, 112, 8910–8922.

(199). Gonzalez MA; Abascal JLF The Shear Viscosity of Rigid Water Models. J. Chem. Phys 2010, 132, 096101–096102. [PubMed: 20210414]

(200). Mao YJ; Zhang YW Prediction of the Temperature-Dependent Thermal Conductivity and Shear Viscosity for Rigid Water Models. J. Nanotechnol. Eng. Med 2012, 3, No. 031009.

(201). Jorgensen WL; Jenson C Temperature Dependence of TIP3P, SPC, and TIP4P Water from NPT Monte Carlo Simulations: Seeking Temperatures of Maximum Density. J. Comput. Chem 1998, 19, 1179–1186.

(202). Lay WK; Miller MS; Elcock AH Correction to Reparameterization of Solute-Solute Interactions for Amino Acid-Sugar Systems Using Isopiestic Osmotic Pressure Molecular Dynamics Simulations. J. Chem. Theory Comput 2017, 13, 3076. [PubMed: 28489366]

(203). Lay WK; Miller MS; Elcock AH Reparameterization of Solute-Solute Interactions for Amino Acid-Sugar Systems Using Isopiestic Osmotic Pressure Molecular Dynamics Simulations. J. Chem. Theory Comput 2017, 13, 1874–1882. [PubMed: 28437100]

(204). Sauter J; Grafmuller A Solution Properties of Hemicellulose Polysaccharides with Four Common Carbohydrate Force Fields. J. Chem. Theory Comput 2015, 11, 1765–1774. [PubMed: 26574386]

(205). Tschampel SM; Kennerty MR; Woods RJ TIP5P-Consistent Treatment of Electrostatics for Biomolecular Simulations. J. Chem. Theory Comput 2007, 3, 1721–1733. [PubMed: 25419191]

(206). Varki A; Gagneux P In Essentials of Glycobiology, 3rd ed.;Varki A, Cummings RD, Esko JD, Stanley P, Hart GW, Aebi M, Darvill AG, Kinoshita T, Packer NH, et al., Eds.; Cold Spring Harbor Laboratory Press: Cold Spring Harbor, NY, 2017; Chapt. 7; https://www.ncbi.nlm.nih.gov/books/NBK453034/.

(207). Patel KR; Roberts JT; Subedi GP; Barb AW Restricted Processing ofCd16a/Fc Gamma Receptor Iiia N-Glycans from Primary Human Nk Cells Impacts Structure and Function. J. Biol. Chem 2018, 293, 3477–3489. [PubMed: 29330305]

(208). Li X; Grant OC; Ito K; Wallace A; Wang S; Zhao P; Wells L; Lu S; Woods RJ; Sharp JS Structural Analysis of the Glycosylated Intact HIV-1 gp120-B12 Antibody Complex Using Hydroxyl Radical Protein Footprinting. Biochemistry 2017, 56, 957–970. [PubMed: 28102671]

(209). Wilhelm D; Behnken HN; Meyer B Glycosylation Assists Binding of HIV Protein gp120 to Human CD4 Receptor. Chem Bio Chem 2012, 13, 524–527.

(210). Grant OC; Smith HM; Firsova D; Fadda E; Woods RJ Presentation, Presentation, Presentation! Molecular-Level Insight into Linker Effects on Glycan Array Screening Data. Glycobiology 2014, 24, 17–25. [PubMed: 24056723]

(211). Lemmin T; Soto C; Stuckey J; Kwong PD Microsecond Dynamics and Network Analysis of the HIV-1 SOSIP Env Trimer Reveal Collective Behavior and Conserved Microdomains of the Glycan Shield. Structure 2017, 25, 1631–1639. [PubMed: 28890362]

(212). Zhou TQ; Doria-Rose NA; Cheng C; Stewart-Jones GBE; Chuang GY; Chambers M; Druz A; Geng H; McKee K; Kwon YD; et al. Quantification of the Impact of the HIV-1-Glycan Shield on Antibody Elicitation. Cell Rep. 2017, 19, 719–732. [PubMed: 28445724]

(213). Qi YF;Jo S; Im W Roles of Glycans in Interactions between gp120 and HIV Broadly Neutralizing Antibodies. Glycobiology 2016, 26, 251–260. [PubMed: 26537503]

(214). Peng W; de Vries RP; Grant OC; Thompson AJ; McBride R; Tsogtbaatar B; Lee PS; Razi N; Wilson IA; Woods RJ; et al. Recent H3n2 Viruses Have Evolved Specificity for Extended, Branched Human-Type Receptors, Conferring Potential for Increased Avidity. Cell Host Microbe 2017, 21, 23–34. [PubMed: 28017661]

(215). Cummings RD; Schnaar RL; Esko JD; Drickamer K; Taylor ME In Essentials of Glycobiology, 3rd ed.;Varki A, Cummings RD, Esko JD, Stanley P, Hart GW, Aebi M, Darvill AG, Kinoshita T, Packer NH, et al., Eds.; Cold Spring Harbor Laboratory Press: Cold Spring Harbor, NY, 2017; Chapt. 29; https://www.ncbi.nlm.nih.gov/books/NBK453057/.

(216). Lee HS; Qi YF; Im W Effects of N-Glycosylation on Protein Conformation and Dynamics: Protein Data Bank Analysis and Molecular Dynamics Simulation Study. Sci. Rep 2015, 5, No. 8926. [PubMed: 25748215]

(217). Joao HC; Scragg IG; Dwek RA Effects of Glycosylation on Protein Conformation and Amide Proton Exchange Rates in RNase B. FEBS Lett. 1992, 307, 343–346. [PubMed: 1322837]

(218). Joao HC; Dwek RA Effects of Glycosylation on Protein Structure and Dynamics in Ribonuclease B and Some of Its Individual Glycoforms. Eur. J. Biochem 1993, 218, 239–244. [PubMed: 8243469]

(219). Nevo N; Thomas L; Chhuon C; Andrzejewska Z; Lipecka J; Guillonneau F; Bailleux A; Edelman A; Antignac C; Guerrera IC Impact of Cystinosin Glycosylation on Protein Stability by Differential Dynamic Stable Isotope Labeling by Amino Acids in Cell Culture (SILAC). Mol. Cell. Proteomics 2017, 16, 457–468. [PubMed: 28082515]

(220). Rudd PM; Joao HC; Coghill E; Fiten P; Saunders MR; Opdenakker G; Dwek RA Glycoforms Modify the Dynamic Stability and Functional Activity of an Enzyme. Biochemistry 1994, 33, 17–22. [PubMed: 8286336]

(221). Wood NT; Fadda E; Davis R; Grant OC; Martin JC; Woods RJ; Travers SA The Influence of N-Linked Glycans on the Molecular Dynamics of the HIV-1 gp120 V3 Loop. PLoS One 2013, 8, e80301. [PubMed: 24303005]

(222). Sang P; Yang LQ; Ji XL; Fu YX; Liu SQ Insight Derived from Molecular Dynamics Simulations into Molecular Motions, Thermodynamics and Kinetics of HIV-1 gp120. PLoS One 2014, 9, No. e104714. [PubMed: 25105502]

(223). Chandramouli B; Chillemi G; Desideri A Structural Dynamics of V3 Loop in a Trimeric Ambiance, a Molecular Dynamics Study on gp120-CD4 Trimeric Mimic. J. Struct. Biol 2014, 186, 132–140. [PubMed: 24583235]

(224). Lee HS; Im W Effects of N-Glycan Composition on Structure and Dynamics of IgG1 Fc and Their Implications for Antibody Engineering. Sci. Rep 2017, 7, No. 12659. [PubMed: 28978918]

(225). Frank M; Walker RC; Lanzilotta WN; Prestegard JH; Barb AW Immunoglobulin G1 Fc Domain Motions: Implications for Fc Engineering. J. Mol. Biol 2014, 426, 1799–1811. [PubMed: 24522230]

(226). Buck PM; Kumar S; Singh SK Consequences of Glycan Truncation on Fc Structural Integrity. mAbs 2013, 5, 904–916. [PubMed: 24492344]

(227). Rudd PM; Dwek RA Glycosylation: Heterogeneity and the 3D Structure of Proteins. Crit. Rev. Biochem. Mol. Biol 1997, 32, 1–100. [PubMed: 9063619]

(228). Gagneux P; Aebi M; Varki A In Essentials of Glycobiology, 3rd ed.;Varki A, Cummings RD, Esko JD, Stanley P, Hart GW, Aebi M, Darvill AG, Kinoshita T, Packer NH, et al., Eds.; Cold Spring Harbor Laboratory Press: Cold Spring Harbor, NY, 2017; Chapt. 20; https://www.ncbi.nlm.nih.gov/books/NBK453067/.

(229). Colley KJ; Varki A; Kinoshita T In Essentials of Glycobiology, 3rd ed.;Varki A, Cummings RD, Esko JD, Stanley P, Hart GW, Aebi M, Darvill AG, Kinoshita T, Packer NH, et al., Eds.; Cold Spring Harbor Laboratory Press: Cold Spring Harbor, NY, 2017; Chapt. 4; https://www.ncbi.nlm.nih.gov/books/NBK453052/.

(230). Khatri K; Klein JA; White MR; Grant OC; Leymarie N; Woods RJ; Hartshorn KL; Zaia J Integrated Omics and Computational Glycobiology Reveal Structural Basis for Influenza A Virus Glycan Microheterogeneity and Host Interactions. Mol. Cell. Proteomics 2016, 15, 1895–1912. [PubMed: 26984886]

(231). Gimeno A; Reichardt NC; Canada FJ; Perkams L; Unverzagt C; Jimenez-Barbero J; Arda A NMR and Molecular Recognition of N-Glycans: Remote Modifications of the Saccharide Chain Modulate Binding Features. ACS Chem. Biol 2017, 12, 1104–1112. [PubMed: 28192664]

(232). Behrens AJ; Vasiljevic S; Pritchard LK; Harvey DJ; Andev RS; Krumm SA; Struwe WB; Cupo A; Kumar A; Zitzmann N; et al. Composition and Antigenic Effects of Individual Glycan Sites of a Trimeric HIV-1 Envelope Glycoprotein. Cell Rep. 2016, 14, 2695–2706. [PubMed: 26972002]

(233). Reading PC; Tate MD; Pickett DL; Brooks AG Glycosylation as a Target for Recognition of Influenza Viruses by the Innate Immune System. Adv. Exp. Med. Biol 2007, 598, 279–292. [PubMed: 17892219]

(234). Job ER; Deng YM; Barfod KK; Tate MD; Caldwell N; Reddiex S; Maurer-Stroh S; Brooks AG; Reading PC Addition of Glycosylation to Influenza A Virus Hemagglutinin Modulates Antibody-Mediated Recognition of H1N1 2009 Pandemic Viruses. J. Immunol 2013, 190, 2169–2177. [PubMed: 23365085]

(235). Herve PL; Lorin V; Jouvion G; Da Costa B; Escriou N Addition of N-Glycosylation Sites on the Globular Head of the H5 Hemagglutinin Induces the Escape of Highly Pathogenic Avian Influenza a H5N1 Viruses from Vaccine-Induced Immunity. Virology 2015, 486, 134–145. [PubMed: 26433051]

(236). Tate MD; Job ER; Deng YM; Gunalan V; Maurer-Stroh S; Reading PC Playing Hide and Seek: How Glycosylation of the Influenza Virus Hemagglutinin Can Modulate the Immune Response to Infection. Viruses 2014, 6, 1294–1316. [PubMed: 24638204]

(237). Chong Teoh T; Heidelberg T; Rizman-Idid M Systematic Protein-Protein Docking and Molecular Dynamics Studies of HIV-1 gp120 and CD4: Insights for New Drug Development. DARU J. Pharm. Sci 2011, 19, 469–475 (https://www.ncbi.nlm.nih.gov/pmc/articles/PMC3436085/).

(238). Stewart-Jones GB; Soto C; Lemmin T; Chuang GY; Druz A; Kong R; Thomas PV; Wagh K; Zhou T; Behrens AJ; et al. Trimeric HIV-1-Env Structures Define Glycan Shields from Clades A, B, and G. Cell 2016, 165, 813–826. [PubMed: 27114034]

(239). McCoy LE; van Gils MJ; Ozorowski G; Messmer T; Briney B; Voss JE; Kulp DW; Macauley MS; Sok D; Pauthner M; et al. Holes in the Glycan Shield of the Native HIV Envelope Are a Target of Trimer-Elicited Neutralizing Antibodies. Cell Rep. 2016, 16, 2327–2338. [PubMed: 27545891]

(240). Bewley CA Solution Structure of a Cyanovirin-N: Man Alpha 1–2man Alpha Complex: Structural Basis for High-Affinity Carbohydrate-Mediated Binding to gp120. Structure 2001, 9, 931–940. [PubMed: 11591348]

(241). Horiya S; MacPherson IS; Krauss IJ Recent Strategies Targeting HIV Glycans in Vaccine Design. Nat. Chem. Biol 2014, 10, 990–999. [PubMed: 25393493]

(242). Garces F; Sok D; Kong L; McBride R; Kim HJ; Saye-Francisco KF; Julien JP; Hua Y; Cupo A; Moore JP; et al. Structural Evolution of Glycan Recognition by a Family of Potent HIV Antibodies. Cell 2014, 159, 69–79. [PubMed: 25259921]

(243). Zhang Y; Niu Y; Tian J; Liu X; Yao X; Liu H The Glycan-Mediated Mechanism on the Interactions of gp120 with CD4 and Antibody: Insights from Molecular Dynamics Simulation. Chem. Biol. Drug Des 2017, 90, 1237–1246. [PubMed: 28632942]

(244). Yang M; Huang J; Simon R; Wang LX; MacKerell AD Jr. Conformational Heterogeneity of the HIV Envelope Glycan Shield. Sci. Rep 2017, 7, No. 4435. [PubMed: 28667249]

(245). Taylor ME; Drickamer K; Schnaar RL; Etzler ME; Varki A In Essentials of Glycobiology, 3rd ed.;Varki A, Cummings RD, Esko JD, Stanley P, Hart GW, Aebi M, Darvill AG, Kinoshita T, Packer NH, et al., Eds.; Cold Spring Harbor Laboratory Press: Cold Spring Harbor, NY, 2017; Chapt. 28; https://www.ncbi.nlm.nih.gov/books/NBK453078/.

(246). Imberty A; Prestegard JH In Essentials of Glycobiology, 3rd ed.;Varki A, Cummings RD, Esko JD, Stanley P, Hart GW, Aebi M, Darvill AG, Kinoshita T, Packer NH, et al., Eds.; Cold Spring Harbor Laboratory Press: Cold Spring Harbor, NY, 2017; Chapt. 30; https://www.ncbi.nlm.nih.gov/books/NBK453078/.

(247). Grant OC; Woods RJ Recent Advances in Employing Molecular Modelling to Determine the Specificity of Glycan-Binding Proteins. Curr. Opin. Struct. Biol 2014, 28, 47–55. [PubMed: 25108191]

(248). Agirre J; Davies G; Wilson K; Cowtan K Carbohydrate Anomalies in the PDB. Nat. Chem. Biol 2015, 11, 303–303. [PubMed: 25885951]

(249). Nivedha AK; Makeneni S; Foley BL; Tessier MB; Woods R J. Importance of Ligand Conformational Energies in Carbohydrate Docking: Sorting the Wheat from the Chaff. J. Comput. Chem 2014, 35, 526–539. [PubMed: 24375430]

(250). Singh A; Kett WC; Severin IC; Agyekum I; Duan J; Amster IJ; Proudfoot AEI; Coombe DR; Woods RJ The Interaction of Heparin Tetrasaccharides with Chemokine CCL5 Is Modulated by Sulfation Pattern and pH. J. Biol. Chem 2015, 290, 15421–15436. [PubMed: 25907556]

(251). Shaw JP; Johnson Z; Borlat F; Zwahlen C; Kungl A; Roulin K; Harrenga A; Wells TN; Proudfoot AE The X-Ray Structure of RANTES: Heparin-Derived Disaccharides Allows the Rational Design of Chemokine Inhibitors. Structure 2004, 12, 2081–2093. [PubMed: 15530372]

(252). Chung CW; Cooke RM; Proudfoot AE; Wells TN The Three-Dimensional Solution Structure of RANTES. Biochemistry 1995, 34, 9307–9314. [PubMed: 7542919]

(253). Joosten RP; Lutteke T Carbohydrate 3D Structure Validation. Curr. Opin. Struct. Biol 2017, 44, 9–17. [PubMed: 27816840]

(254). Lütteke T; von der Lieth C-W Data Mining the PDB for Glyco-Related Data. Methods Mol. Biol 2009, 534, 293–310. [PubMed: 19277543]

(255). Sapay N; Nurisso A; Imberty A Simulation of Carbohydrates, from Molecular Docking to Dynamics in Water. Methods Mol. Biol 2013, 924, 469–483. [PubMed: 23034760]

(256). Nivedha AK; Thieker DF; Makeneni S; Hu H; Woods RJ Vina-Carb: Improving Glycosidic Angles During Carbohydrate Docking. J. Chem. Theory Comput 2016, 12, 892–901. [PubMed: 26744922]

(257). Janin J; Henrick K; Moult J; Ten Eyck L; Sternberg MJE; Vajda S; Vakser I; Wodak SJ Capri: A Critical Assessment of Predicted Interactions. Proteins: Struct., Funct., Bioinf 2003, 52, 2–9.

(258). Weichenberger CX; Sippl MJ NQ-Flipper: Recognition and Correction of Erroneous Asparagine and Glutamine Side-Chain Rotamers in Protein Structures. Nucleic Acids Res. 2007, 35, W403–W406. [PubMed: 17478502]

(259). Baumgartner MP; Camacho CJ Choosing the Optimal Rigid Receptor for Docking and Scoring in the Csar 2013/2014 Experiment. J. Chem. Inf. Model 2016, 56, 1004–1012. [PubMed: 26222931]

(260). Kokh DB; Wade RC; Wenzel W Receptor Flexibility in Small-Molecule Docking Calculations. WIREs Comput. Mol. Sci 2011, 1, 298–314.

(261). Labonte JW; Adolf-Bryfogle J; Schief WR; Gray JJ Residue-Centric Modeling and Design of Saccharide and Glycoconjugate Structures. J. Comput. Chem 2017, 38, 276–287. [PubMed: 27900782]

(262). Hudson KL; Bartlett GJ; Diehl RC; Agirre J; Gallagher T; Kiessling LL; Woolfson DN Carbohydrate-Aromatic Interactions in Proteins. J. Am. Chem. Soc 2015, 137, 15152–15160. [PubMed: 26561965]

(263). Asensio JL; Arda A; Canada FJ; Jimenez-Barbero J Carbohydrate-Aromatic Interactions. Acc. Chem. Res 2013, 46, 946–954. [PubMed: 22704792]

(264). Hsu CH; Park S; Mortenson DE; Foley BL; Wang X; Woods RJ; Case DA; Powers ET; Wong CH; Dyson HJ; et al. The Dependence of Carbohydrate-Aromatic Interaction Strengths on the Structure of the Carbohydrate. J. Am. Chem. Soc 2016, 138, 7636–7648. [PubMed: 27249581]

(265). Mishra SK; Adam J; Wimmerova M; Koca J In Silico Mutagenesis and Docking Study of *Ralstonia solanacearum* RSL Lectin: Performance of Docking Software to Predict Saccharide Binding. J. Chem. Inf. Model 2012, 52, 1250–1261. [PubMed: 22506916]

(266). Agostino M; Jene C; Boyle T; Ramsland PA; Yuriev E Molecular Docking of Carbohydrate Ligands to Antibodies: Structural Validation against Crystal Structures. J. Chem. Inf. Model 2009, 49, 2749–2760. [PubMed: 19994843]

(267). Nurisso A; Kozmon S; Imberty A Comparison of Docking Methods for Carbohydrate Binding in Calcium-Dependent Lectins and Prediction of the Carbohydrate Binding Mode to Sea Cucumber Lectin CEL-III. Mol. Simul 2008, 34, 469–479.

(268). Kerzmann A; Fuhrmann J; Kohlbacher O; Neumann D BALLDock/SLICK: A New Method for Protein-Carbohydrate Docking. J. Chem. Inf. Model 2008, 48, 1616–1625. [PubMed: 18646839]

(269). Gauto DF; Di Lella S; Estrin DA; Monaco HL; Marti MA Structural Basis for Ligand Recognition in a Mushroom Lectin: Solvent Structure as Specificity Predictor. Carbohydr. Res 2011, 346, 939–948. [PubMed: 21453906]

(270). Saenger W Structure and Dynamics of Water Surrounding Biomolecules. Annu. Rev. Biophys. Biophys. Chem 1987, 16, 93–114. [PubMed: 3297093]

(271). Gauto DF; Petruk AA; Modenutti CP; Blanco JI; Di Lella S; Martí MA Solvent Structure Improves Docking Prediction in Lectin-Carbohydrate Complexes. Glycobiology 2013, 23, 241–258. [PubMed: 23089616]

(272). Makeneni S; Ji Y; Watson DC; Young NM; Woods RJ Predicting the Origins of Anti-Blood Group Antibody Specificity: A Case Study of the ABO A- and B-Antigens. Front. Immunol 2014, 5, No. 397. [PubMed: 25202309]

(273). Marchetti R; Perez S; Arda A; Imberty A; Jimenez-Barbero J; Silipo A; Molinaro A “Rules of Engagement” of Protein-Glycoconjugate Interactions: A Molecular View Achievable by Using NMR Spectroscopy and Molecular Modeling. Chemistry Open 2016, 5, 274–296. [PubMed: 27547635]

(274). Vyas NK; Vyas MN; Chervenak MC; Johnson MA; Pinto BM; Bundle DR; Quiocho FA Molecular Recognition of Oligosaccharide Epitopes by a Monoclonal Fab Specific for *Shigella flexneri* Y Lipopolysaccharide: X-Ray Structures and Thermodynamics. Biochemistry 2002, 41, 13575–13586. [PubMed: 12427018]

(275). Grant OC; Tessier MB; Meche L; Mahal LK; Foley BL; Woods RJ Combining 3D Structure with Glycan Array Data Provides Insight into the Origin of Glycan Specificity. Glycobiology 2016, 26, 772–783. [PubMed: 26911287]

(276). Kletter D; Singh S; Bern M; Haab BB Global Comparisons of Lectin-Glycan Interactions Using a Database of Analyzed Glycan Array Data. Mol. Cell. Proteomics 2013, 12, 1026–1035. [PubMed: 23399549]

(277). Xuan P; Zhang Y; Tzeng T.-r. J.; Wan X-F; Luo FA Quantitative Structure-Activity Relationship (QSAR) Study on Glycan Array Data to Determine the Specificities of Glycan-Binding Proteins. Glycobiology 2012, 22, 552–560. [PubMed: 22156918]

(278). Oyelaran O; Gildersleeve JC Glycan Arrays: Recent Advances and Future Challenges. Curr. Opin. Chem. Biol 2009, 13, 406–413. [PubMed: 19625207]

(279). Drickamer K; Taylor ME Glycan Arrays for Functional Glycomics. Genome Biology 2002, 3, No. reviews1034.1. [PubMed: 12537579]

(280). Grant OC; Xue X; Ra D; Khatamian A; Foley BL; Woods RJ Gly-Spec: A Webtool for Predicting Glycan Specificity by Integrating Glycan Array Screening Data and 3D Structure. Glycobiology 2016, 26, 1027–1028. [PubMed: 28120784]

(281). Rasmussen TD; Ren PY; Ponder JW; Jensen F Force Field Modeling of Conformational Energies: Importance of Multipole Moments and Intramolecular Polarization. Int. J. Quantum Chem 2007, 107, 1390–1395.

(282). Friesner RA Modeling Polarization in Proteins and ProteinLigand Complexes: Methods and Preliminary Results. Adv. Protein Chem 2005, 72, 79–104. [PubMed: 16581373]

(283). Cieplak P; Dupradeau F-Y; Duan Y; Wang J Polarization Effects in Molecular Mechanical Force Fields. J. Phys.: Condens. Matter 2009, 21, 333102. [PubMed: 21828594]

(284). Zhang P; Bao P; Gao J Dipole Preserving and Polarization Consistent Charges. J. Comput. Chem 2011, 32, 2127–2139. [PubMed: 21541954]

(285). Patel S; Mackerell AD; Brooks CL CHARMM Fluctuating Charge Force Field for Proteins: II - Protein/Solvent Properties from Molecular Dynamics Simulations Using a Nonadditive Electrostatic Model. J. Comput. Chem 2004, 25, 1504–1514. [PubMed: 15224394]

(286). Anisimov VM; Lamoureux G; Vorobyov IV; Huang N; Roux B; MacKerell AD Determination of Electrostatic Parameters for a Polarizable Force Field Based on the Classical Drude Oscillator. J. Chem. Theory Comput. 2005, 1, 153–168. [PubMed: 26641126]

(287). Elking D; Darden TA; Woods RJ Gaussian Induced Dipole Polarization Model. J. Comput. Chem 2007, 28, 1261–1274. [PubMed: 17299773]

(288). Woods RJ; Dwek RA; Edge CJ; Fraser-Reid B Molecular Mechanical and Molecular Dynamical Simulations of Glycoproteins and Oligosaccharides. 1. GLYCAM_93 Parameter Development. J. Phys. Chem 1995, 99, 3832–3846.

(289). Sattelle BM; Almond A Shaping up for Structural Glycomics: A Predictive Protocol for Oligosaccharide Conformational Analysis Applied to N-Linked Glycans. Carbohydr. Res 2014, 383, 34–42. [PubMed: 24252626]

(290). Galindo-Murillo R; Roe DR; Cheatham TE 3rd Convergence and Reproducibility in Molecular Dynamics Simulations of the DNA Duplex d(GCACGAACGAACGAACGC). Biochim. Biophys. Acta, Gen. Subj 2015, 1850, 1041–1058.

(291). Taha HA; Castillo N; Roy PN; Lowary TL Conformational Studies of Methyl β-D-Arabinofuranoside Using the AMBER/Glycam Approach. J. Chem. Theory Comput 2009, 5, 430–438. [PubMed: 26610115]

(292). Piepenbrink KH; Lillehoj E; Harding CM; Labonte JW; Zuo XT; Rapp CA; Munson RS; Goldblum SE; Feldman MF; Gray JJ; et al. Structural Diversity in the Type IV Pili of Multidrug-resistant Acinetobacter. J. Biol. Chem 2016, 291, 22924–22935. [PubMed: 27634041]

(293). Hambly D; Gross M Laser Flash Photochemical Oxidation to Locate Heme Binding and Conformational Changes in Myoglobin. Int. J. Mass Spectrom 2007, 259, 124–129.

(294). Zhang Y; Wecksler AT; Molina P; Deperalta G; Gross ML Mapping the Binding Interface of VEGF and a Monoclonal Antibody Fab-1 Fragment with Fast Photochemical Oxidation of Proteins (FPOP) and Mass Spectrometry. J. Am. Soc. Mass Spectrom 2017, 28, 850–858. [PubMed: 28255747]

(295). Lee JH; Ozorowski G; Ward AB Cryo-EM Structure of a Native, Fully Glycosylated, Cleaved HIV-1 Envelope Trimer. Science 2016, 351, 1043–1048. [PubMed: 26941313]

(296). Lyumkis D; Julien J-P; de Val N; Cupo A; Potter CS; Klasse P-J; Burton DR; Sanders RW; Moore JP; Carragher B; et al. Cryo-EM Structure of a Fully Glycosylated Soluble Cleaved HIV-1 Envelope Trimer. Science 2013, 342, 1484–1490. [PubMed: 24179160]

(297). Amon R; Grant OC; Leviatan Ben-Arye S; Makeneni S; Nivedha AK; Marshanski T; Norn C; Yu H; Glushka JN; Fleishman SJ; et al. A Combined Computational-Experimental Approach to Define the Structural Origin of Antibody Recognition of Sialyl-Tn, a Tumor-Associated Carbohydrate Antigen. Sci. Rep 2018, 8, 10786. [PubMed: 30018351]

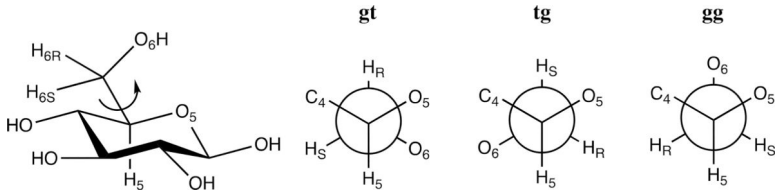

Figure 1.
Rotamer definitions for the C5-C6 bond in pyranoses.

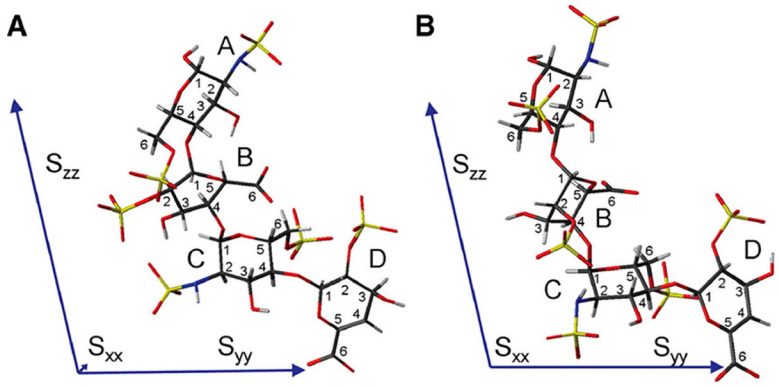

Figure 2.

Orientation of the principal axis frame of the order tensor relative to the structure of a tetrasaccharide fragment of heparin with ring B in (A) $^{2}S_{0}$ conformation and (B) $^{1}C_{4}$ conformation. Reprinted with permission from ref 82. Copyright 2009 Oxford University Press.

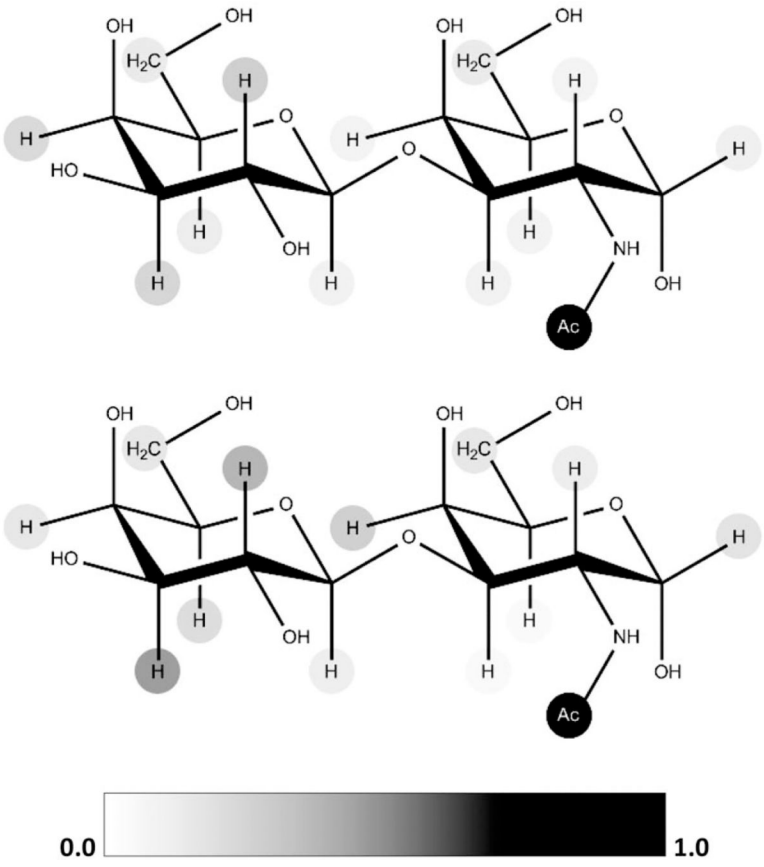

Figure 3.

Normalized NMR-STD data for the Thompson—Friedenreich (TF, Galβ1 — 3GalNAcα) disaccharide cancer antigen complexed with an anti-TF antibody: experimental (upper) and theoretical (lower) intensities are shown as circles, with fill density proportional to the normalized intensity. Reprinted from ref 111. Public Library of Science 2013, licensed under CC BY 4.0.

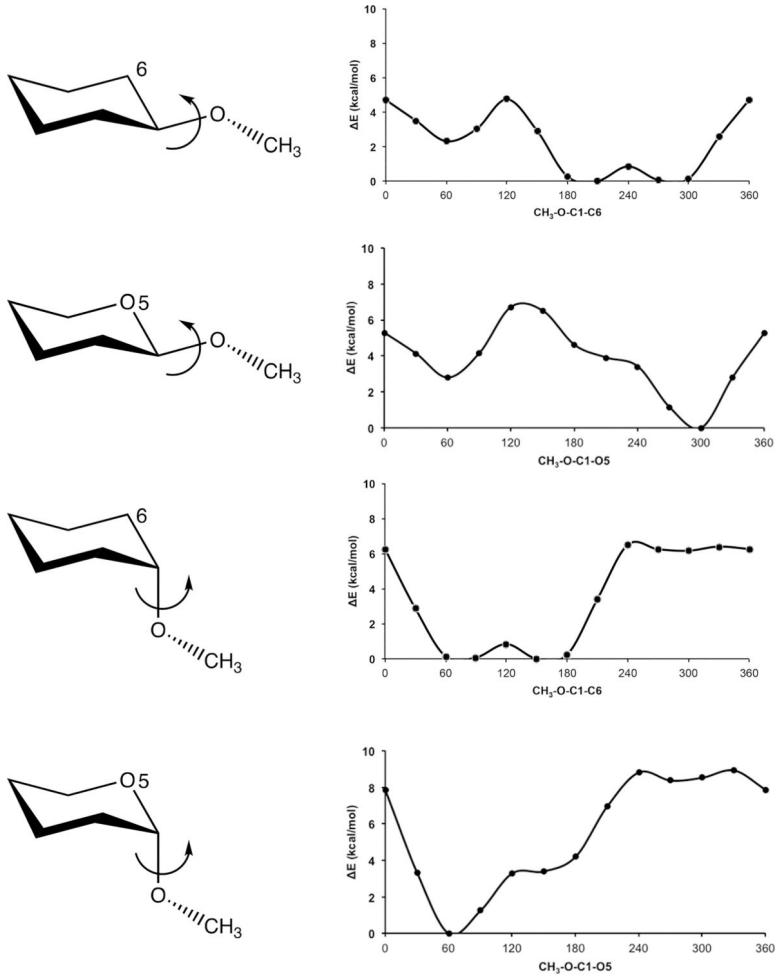

Figure 4.

Bond rotational energies computed at the QM B3LYP/6–31G(2d,2p)//B3LYP/6–31G(2d,2p) level for equatorial and axial 2-OMe-THP and their cyclohexyl analogues, indicating only one dominant energy minimum in the 2-OMe-THP variants, due to the presence of the exoanomeric effect in these analogues.

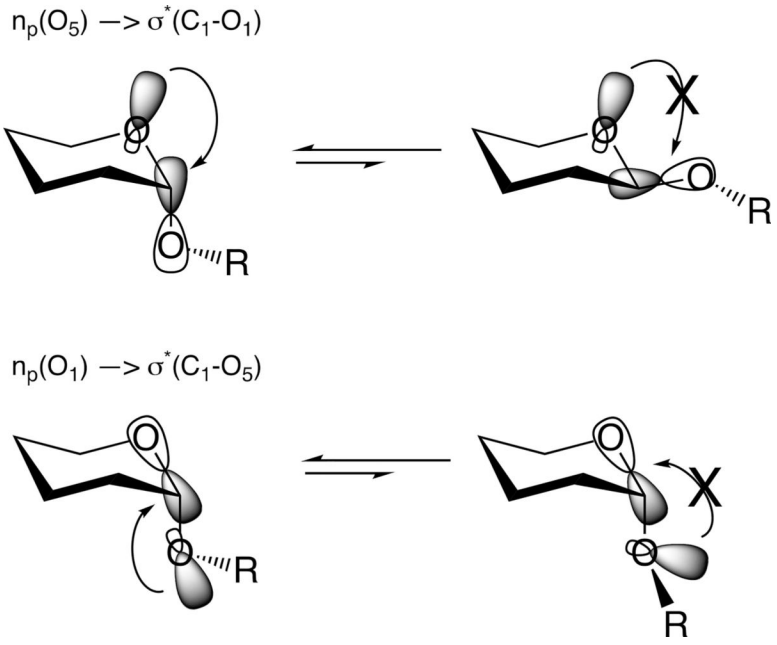

Figure 5.
Electronic origin [$n_p(O) \rightarrow \sigma^*(C\text{-}O)$] of (top) the endoanomeric effect and (bottom) the exoanomeric effect.

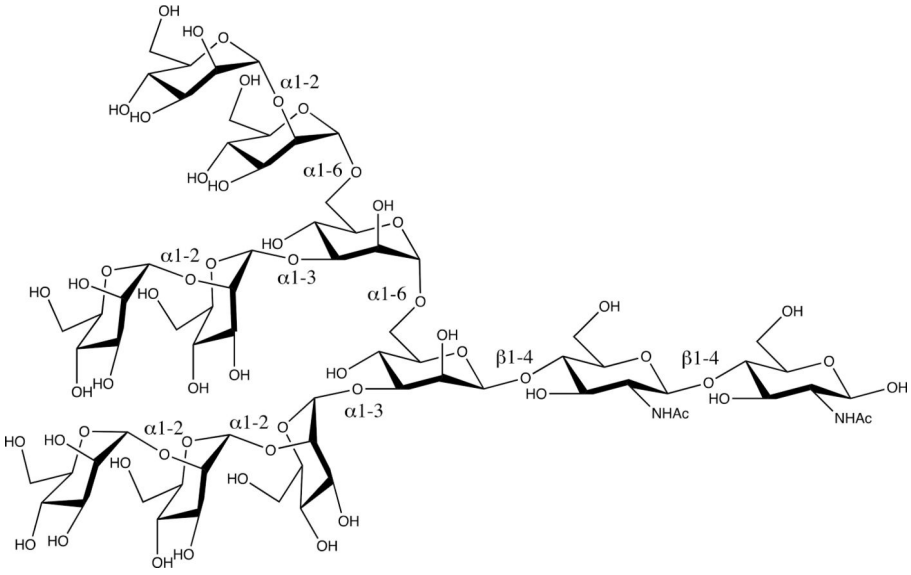

Figure 6.

Schematic representation of the high-mannose oligosaccharide $Man_9GlcNAc_2$, indicating the two 1–6 linkages that each contain three bonds.

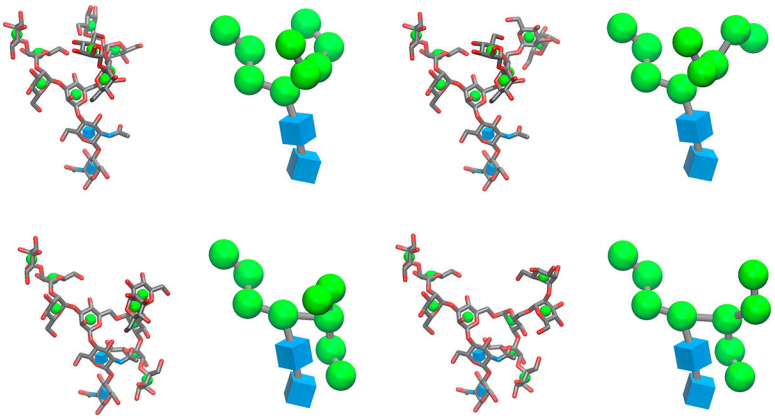

Figure 7.

Four stable conformers[9,144] of a high-mannose glycan ($Man_9GlcNAc_2$, Man-9) generated by use of GLYCAM-Web (www.glycam.org), displayed in 3D-SNFG icon mode (left) and full 3D-SNFG mode (right), where SNFG is symbol nomenclature for glycans. Upper row inner/outer 1–6 linkage conformations shown are gg/gg (top left), gg/gt (top right), gt/gg (bottom left), and gt/gt (bottom right). In the 3D-SNFG representations, mannopyranose is shown as a green sphere and *N*-acetylglucopyranosamine is shown as a blue cube.[145,146] Images were generated with Visual Molecular Dynamics (VMD),[147] using the 3D-SNFG plug-in available at www.glycam.org/3d-snfg.

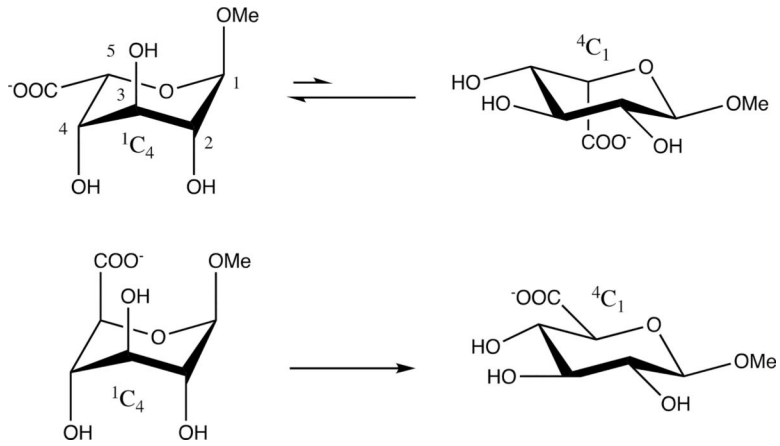

Figure 8.

$^1C_4$ structure of IdoA (upper left) is dominant in solution[117] despite the presence of two destabilizing 1–3 diaxial oxygen groups. In contrast, GlcA (lower) prefers exclusively the $^4C_1$ structure.

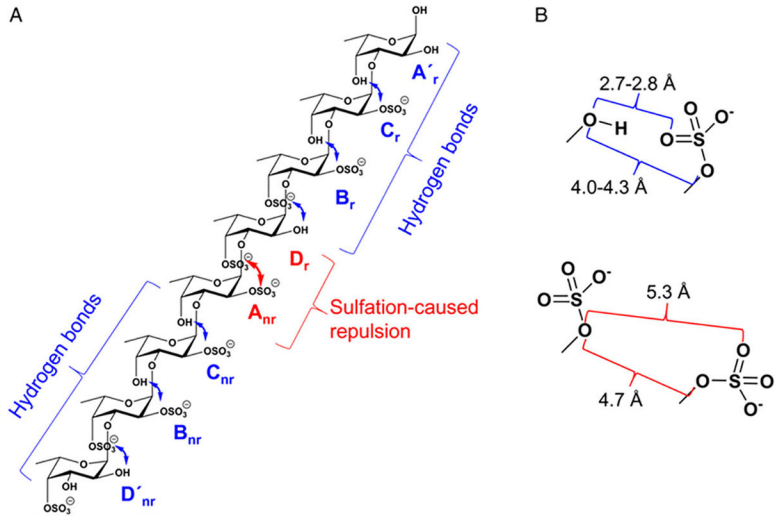

Figure 9.

(A) Schematic representation explaining the sulfation pattern-related hydrogen bonds (in blue) and repulsive effects (in red) in a fucan octasaccharide. (B) Atomic distances between neighboring residue interactions. Reprinted with permission from ref 152. Copyright 2009 Oxford University Press.

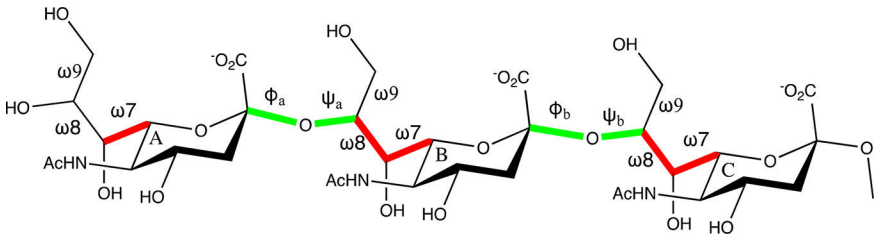

Figure 10.

Trisaccharide fragment of 2—8-linked poly(sialic acid) (PSA), with the highly inflexible ω angles shown in red and the potentially flexible ϕ and Ψ angles shown in green.

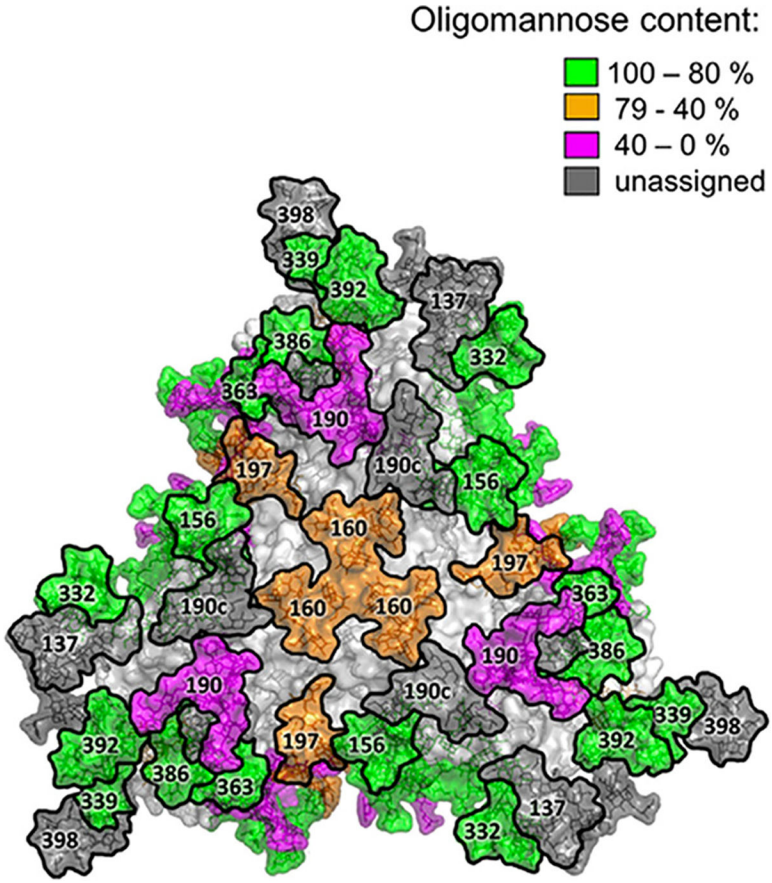

Figure 11.

Site-specific glycosylation profiles for HIV gp120/gp41 trimer antigen. Reprinted from ref 232. Elsevier 2016, licensed under CC BY 4.0.

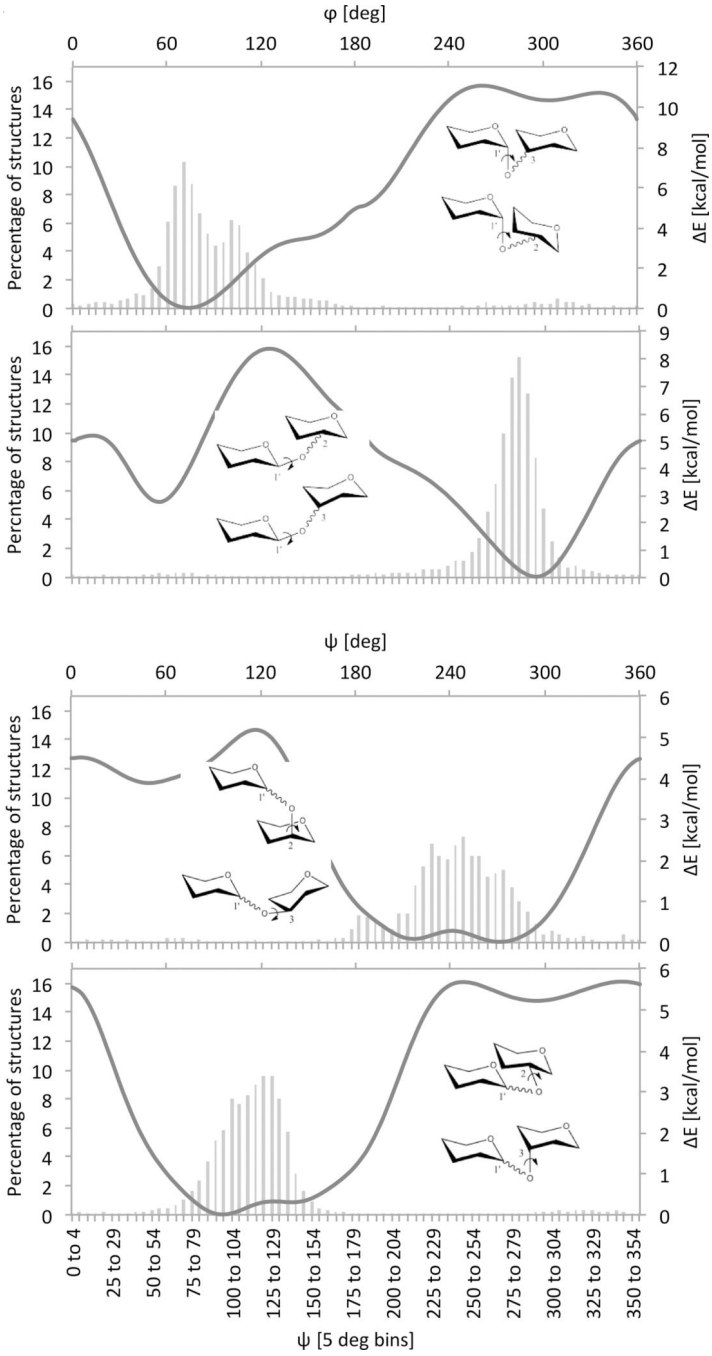

Figure 12.

Comparison of average energies for glycosidic torsion rotation for the ϕ and Ψ angles in model disaccharides (solid lines) to the glycosidic torsion angle distributions of carbohydrates from experimental cocrystal structures (histograms).[249]

Table 1.

NMR-Based and Computed Populations for Interresidue Torsion Angles in Fragments of PSA Trisialoside α-Neu5Ac-(2–8)-α-Neu5Ac-(2–8)-α-Neu5Ac-OMe (a-b-c)[65]

	+gauche/trans/-gauche populations (%)	
linkage	**by NMR**	**by MD (100 ns)**
	ω7 Angle	
terminal a	100/0/0	100/0/0
internal b	100/0/0	100/0/0
	ω 8 Angle	
internal c	100/0/0	100/0/0
terminal a	0/100/0	15/74/7
	ω9 Angle 60/25/0	
internal b	60/25/0	70/30/0
internal c	66/31/0	89/11/0